AD-753 909

DYNAMICS OF CABLES TOWED FROM AIRCRAFT

James G. R. Hansen, et al
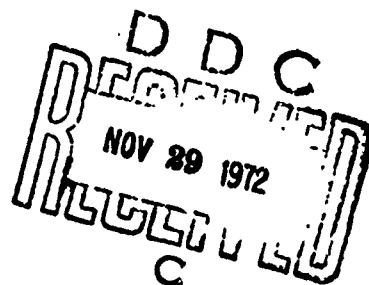
Air Force Academy
Air Force Academy, Colorado

October 1972

DYNAMICS OF CABLES TOWED FROM AIRCRAFT

by

CAPTAIN JAMES G. R. HANSEN
CAPTAIN STEVEN A. CRIST

RESEARCH REPORT 72-8
OCTOBER 1972

UNITED STATES AIR FORCE ACADEMY
COLORADO 80840

DOCUMENT CONTROL DATA - R & D

Security classification of title, body of abstract and indexing annotation must be entered when the overall report is classified)

1 ORIGINATING ACTIVITY (Corporate author)	2a. REPORT SECURITY CLASSIFICATION
Hq USAFA (Faculty Secretariat) USAF Academy, Colorado 80840	Unclassified
	2b. GROUP

3 REPORT TITLE

DYNAMICS OF CABLES TOWED FROM AIRCRAFT

4 DESCRIPTIVE NOTES (Type of report and inclusive dates)
Research Report

5 AUTHOR(S) (First name, middle initial, last name)
Captain James G. R. Hansen
Captain Steven A. Crist

6 REPORT DATE	7a. TOTAL NO. OF PAGES	7b. NO. OF REFS
October 1972	81 93	6
8a. CONTRACT OR GRANT NO.	9a. ORIGINATOR'S REPORT NUMBER(S)	
b. PROJECT NO.	RR 72-8	
c.	9b. OTHER REPORT NO(S) (Any other numbers that may be assigned this report)	
d.	None	

10 DISTRIBUTION STATEMENT

Distribution of this document is unlimited

11 SUPPLEMENTARY NOTES	12. SPONSORING MILITARY ACTIVITY
	Faculty Secretariat (DFSS) USAF Academy, Colorado 80840

13 ABSTRACT

This report describes a "lumped mass" computer simulation of a trailing wire system towed by an orbiting aircraft. The USAF U-10 aircraft flight conditions were used as applied to three flightpaths: (1) Constant altitude circular, (2) Constant altitude elliptical, (3) Non-constant altitude circular orbit. These flightpaths were flown in no wind and 30 knot wind conditions.

Wire lengths of 4000 ft and 8000 ft were used where the free end was attached to a circular sphere of 25 and 100 lbs.

The results from 12 orbiting trailing wire configurations are tabulated and/or plotted. One of the main objectives in this analysis was to determine how yo-yo of the free end of the wire in wind might be alleviated or at least minimized.

iA

DD FORM 1473 1 NOV 65

DYNAMICS OF CABLES TOWED FROM AIRCRAFT

by

Captain James G. R. Hansen
Captain Steven A. Crist

iB

Editorial Review by Captain John B. McTasney
Department of English

ic

ACKNOWLEDGMENTS

ABSTRACT

This report describes a "lumped mass" computer simulation of
a trailing wire system towed by an orbiting aircraft. The USAF U-10
aircraft flight conditions were used as applied to three flightpaths:
(1) Constant altitude circular, (2) Constant altitude elliptical,
(3) Non-constant altitude circular orbit. These flightpaths were
flown in no wind and 30 knot wind conditions.

Wire lengths of 4000 ft and 8000 ft were used where the free
end was attached to a circular sphere of 25 and 100 lbs.

The results from 12 orbiting trailing wire configurations are
tabulated and/or plotted. One of the main objectives in this analysis
was to determine how yo-yo of the free end of the wire in wind might
be alleviated or at least minimized.

TABLE OF CONTENTS

LIST OF FIGURES

LIST OF FIGURES
(Continued)

LIST OF TABLES

LIST OF SYMBOLS

A   Platform area of cable segment

C_D Aerodynamic drag coefficient

C_L Aerodynamic lift coefficient

D   Aerodynamic drag

e   Stretched spring length

g   Acceleration of gravity

h   Aircraft altitude

k   Spring constant

L   Aerodynamic lift

m   Mass

N   Number of lumped masses

q   Dynamic pressure

$\bar{R}$ Aircraft position vector

s_o Unstretched spring length

TSTEP   Time step of Runge-Kutta integration scheme

V_a Relative aircraft speed

V_t Aircraft ground track speed

V_w Wind speed

x   X position coordinate

y   Y position coordinate

z   Z position coordinate

α Angle of attack

LIST OF SYMBOLS
(Continued)

η Direction cosine of unit vector in lift direction

σ Angle separating V_t from positive Y axis

λ Aircraft bank angle

ξ Direction cosine of unit vector in drag direction

τ Period of vibration

$\dot{\phi}$ Aircraft angular velocity

ψ Angle separating $\overline{R}$ from positive X axis

INTRODUCTION

An orbiting trailing wire system consists of an aircraft flying in a closed path and towing a long cable. The shape and size of the orbit of the free end of the cable are of prime importance. More specifically, the yo-yo, or vertical oscillation of the free end, must be controlled within certain limits if the trailing wire system is to be useful.

This paper describes a computer simulation of the system, in which the cable is modeled by a series of lumped masses connected together by linear, massless springs. The coupled, second order differential equations of motion of the lumped masses are programmed onto a digital computer. This paper uses the computer simulation to study the steady state motion of the cable with primary emphasis given to the motion of the endpoint of the cable. Since there are only a finite number of mass points in the model, errors are introduced into the analysis. However, these errors are insignificant even if relatively few mass points are taken.

Any orbiting trailing wire system can be analyzed with the computer simulation. This paper contains the analysis of a specific trailing wire system referred to as the SNOWBIRD system. The SNOWBIRD system has been flight tested by Air Force Academy personnel using a U-10 as the towing aircraft and a cone attached to the end of the

cable. The cable in the computer simulation is the same cable that has been flight tested. During the simulation the aircraft is flown at a velocity and a bank angle used by the U-10 in flight tests.

PROGRAMMING THE EQUATIONS OF MOTION

2.1 Description of Lumped Mass Model

The orbiting trailing wire is modeled by a series of lumped masses connected together by linear, massless springs. Figure 1 is the model of a trailing wire cable approximated by 10 masses and 10 identical linear, massless springs. The leading end of the cable, or Station 1, represents the towing aircraft. One-tenth of the total mass of the cable is located at each of the 10 lumped masses, Stations 2 thru 11. The mass of the drogue is included in the final lumped mass, Station 11.

The equations of motion for the trailing wire's masses are developed in Appendix I of this paper. The three equations of motion for mass point i are:

$$m_i \ddot{x}_i = k_i \left(1 - \frac{S_{o_i}}{e_i}\right)(x_{i+1} - x_i) - k_{i-1}\left(1 - \frac{S_{o_i}}{e_{i-1}}\right)(x_i - x_{i-1})$$

$$+ L_i \eta_{x_i} + L_{i-1} \eta_{x_{i-1}} + (D_i + D_{i-1})\xi_{x_i}$$

$$m_i \ddot{y}_i = k_i \left(1 - \frac{S_{o_i}}{e_o}\right)(y_{i+1} - y_i) - k_{i-1}\left(1 - \frac{S_{o_i}}{e_{i-1}}\right)(y_i - y_{i-1})$$

$$+ L_i \eta_{y_i} + L_{i-1} \eta_{y_{i-1}} + (D_i + D_{i-1})\xi_{y_i}$$

2
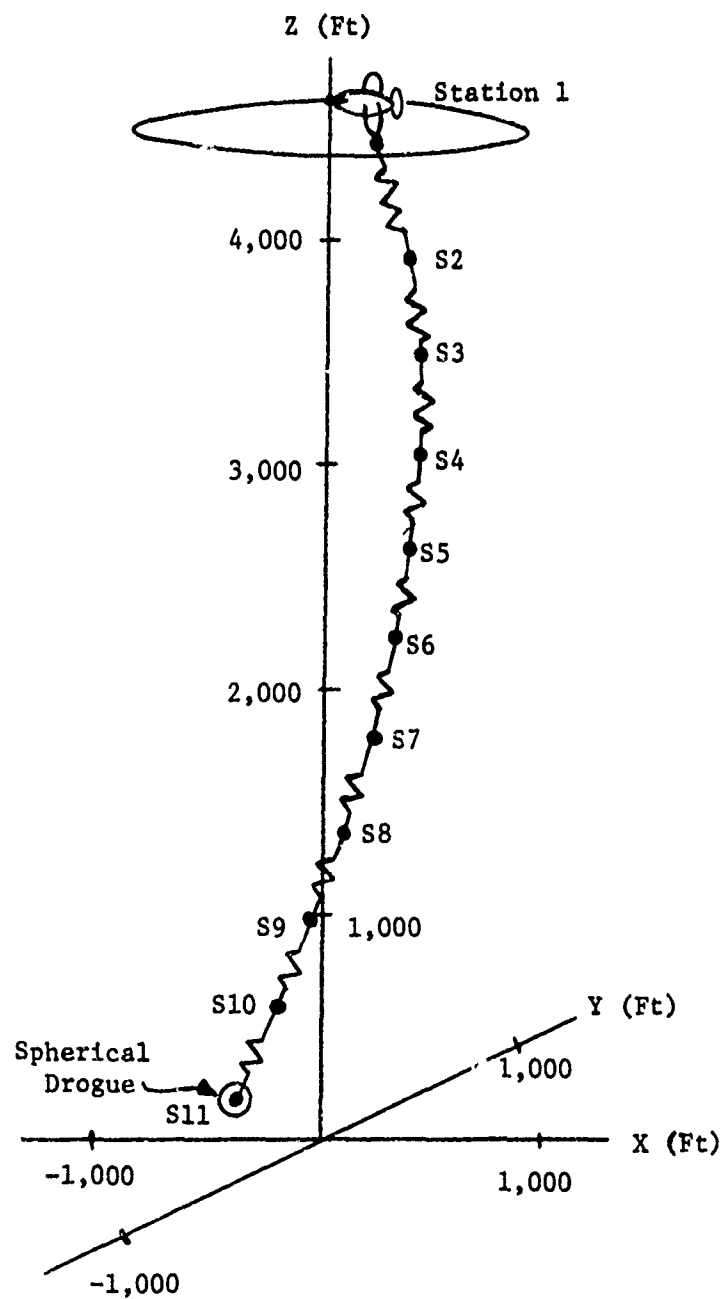
FIGURE 1

LUMPED MASS MODEL OF TRAILING WIRE SYSTEM

$$m_i \ddot{z}_i = k_i \left(1 - \frac{S_{o_i}}{e_i}\right)(z_{i+1} - z_i) - k_{i-1}\left(1 - \frac{S_{o_i}}{e_{i-1}}\right)(z_i - z_{i-1})$$

$$- m_i g + L_i \eta_{z_i} + L_{i-1} \eta_{z_{i-1}} + (D_i + D_{i-1}) \xi_{z_i}$$

where: m_i = mass of ith point

k_i = spring constant for segment i

e_i = stretched spring length

S_{o_i} = unstretched spring length

L_i = aerodynamic lift

D_i = aerodynamic drag

g = acceleration of gravity

η_{x_i}, η_{y_i}, η_{z_i} are direction cosines of $\overline{\eta}$, the unit vector

in the lift direction

ξ_{x_i}, ξ_{y_i}, and ξ_{z_i} are direction cosines of $\overline{\xi}$, the unit vector

in the drag direction.

During each step of the integration of the equations of motion, the aircraft is flown an incremental distance and the equations are integrated using a Runge-Kutta routine. The displacement of the aircraft enters into the three equations of motion for the mass point immediately below the aircraft, or at Station 2.

2.2 Aircraft Orbit

The towing aircraft is programmed to fly in either a circular or an elliptical orbit. The velocity of the aircraft is constant with respect to the wind. Thus, as the aircraft is flown in an orbit, the pilot only has to vary the bank angle and direction of flight of the aircraft. If the aircraft was programmed to fly with a constant ground track velocity in a prevailing wind, the pilot would have to continually adjust the throttle in addition to the bank angle and direction as the aircraft progressed around its orbit. Such a maneuver would have the detrimental effect of increasing the yo-yo motion of the drogue, as noted in Case 3 of Section 4.2a.

The relative velocity of the aircraft is the vector summation of the ground track velocity of the aircraft and the negative of the wind velocity. shows this vector summation at various points along a constant altitude circular orbit. (In order to simplify terminology, an orbit will henceforth be assumed to be flown at a constant altitude unless stated otherwise.) The ground track velocity is tangent to the orbit, and the angle θ separates this velocity from the positive Y axis. The angle ψ separates the aircraft position vector from the positive X axis. The vector equations needed to solve for the ground track velocity are:

$$\overline{V}_w = - V_w \overline{i}$$

$$\overline{V}_t = - V_t \sin\theta \; \overline{i} + V_t \cos\theta \; \overline{j} \; .$$
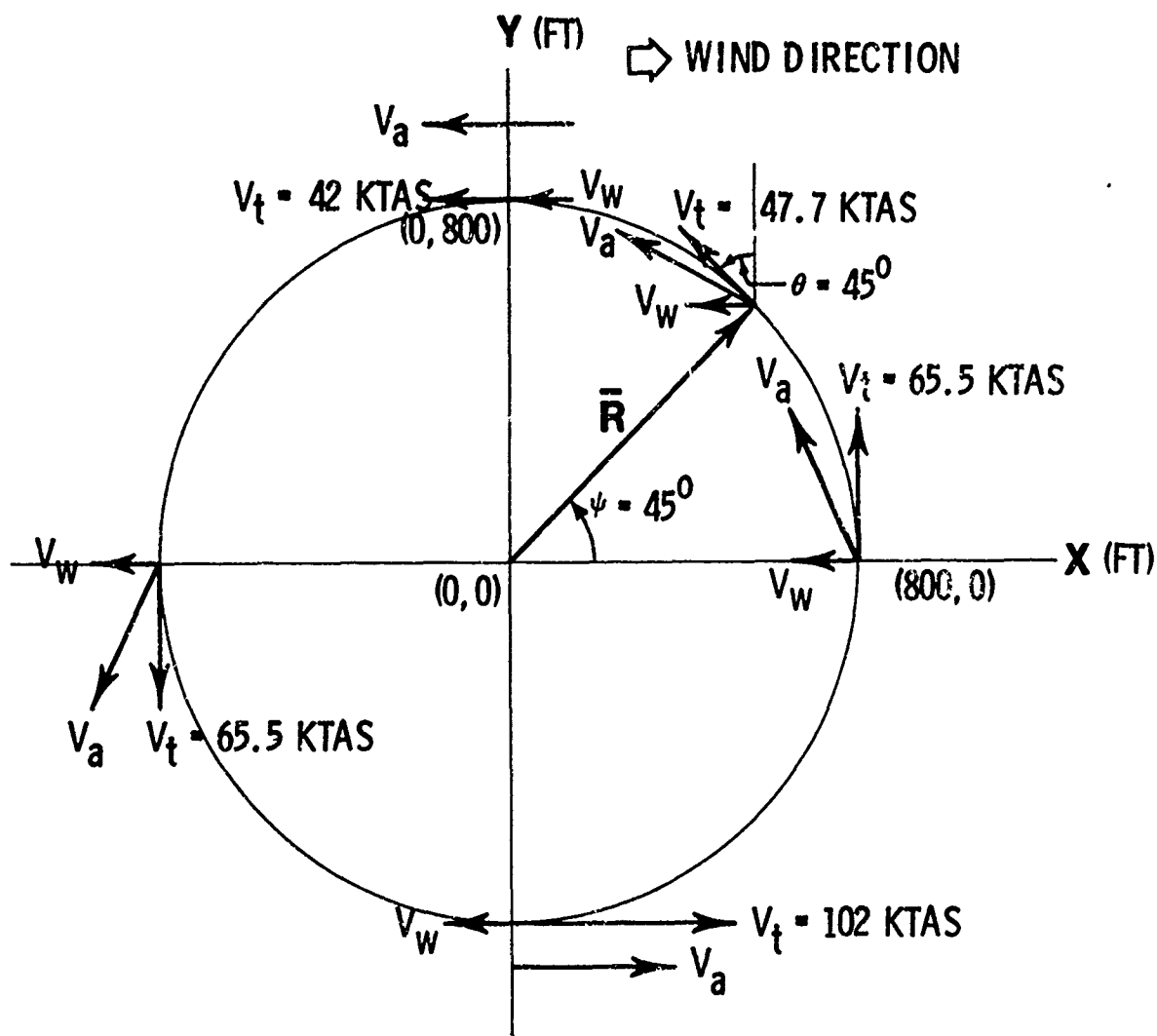
5

FIGURE 2

AIRCRAFT CIRCULAR ORBIT

V_W = WIND SPEED = 30 KTAS

V_a = AIRCRAFT RELATIVE SPEED = 72 KTAS

V_t = AIRCRAFT GROUND TRACK SPEED

$\bar{R}$ = AIRCRAFT POSITION VECTOR

The resultant of these two vectors is:

$$\overline{V}_a = \overline{V}_w + \overline{V}_t = (-V_w - V_t \sin\theta)\overline{i} + V_t \cos\theta \, \overline{j} \; .$$

Taking the magnitude of each side of the above vector equation yields the quadratic equation:

$$V_t^2 + (2V_w \sin\theta)V_t + (V_w^2 - V_a^2) = 0 \; .$$

The wind speed, V_w, and the relative aircraft speed, V_a, are specified for a particular flight test. The quadratic equation is solved for the unknown, V_t. The equation for V_t is programmed in the computer subroutine that "flies the aircraft". Once $\overline{V}_t$ is calculated, the aircraft is flown at this ground track velocity for an in incremental time step. At each new aircraft location $\overline{V}_t$ is recalculated, and in this manner the aircraft proceeds around the orbit.

If the aircraft flies in an elliptical orbit, the same equation for V_t is derived. Figure 3 shows the vector summation of $\overline{V}_t$ and $\overline{V}_w$ at various points along an elliptical orbit. The main difference between the analysis of elliptical and circular orbits is that the angles ψ and θ are equal for a circular orbit but not equal for an elliptical orbit. For a circular orbit $\theta = \tan^{-1}(y/x)$. For an elliptical orbit $\theta = \cot^{-1}(dy/dx)$.

A non-constant altitude aircraft orbit has been proposed as a method of reducing yo-yo motion of the drogue (Crouch, Baver, Kahle, 1970, p. 36). When properly modified, a constant altitude circular

7

Y (FT)

V_a ←

$V_t = 42$ KTAS ←
(0, 1200)

☐⇒ WIND DIRECTION

V_w ←

V_a $V_t = 54.5$ KTAS
$\theta = 24^0$

V_w ←

$\bar{R}$

V_a $V_t = 65.5$ KTAS

$\dot{\psi} = 45^0$

V_w ←
(0, 0)

V_w ← (800, 0)   **X** (FT)

V_w ←

V_a $V_t = 65.5$ KTAS

V_w ← $V_t = 102$ KTAS

V_a

V_w = WIND SPEED =
       30 KTAS

V_a = AIRCRAFT RELATIVE SPEED =
       72 KTAS

V_t = AIRCRAFT GROUND TRACK SPEED

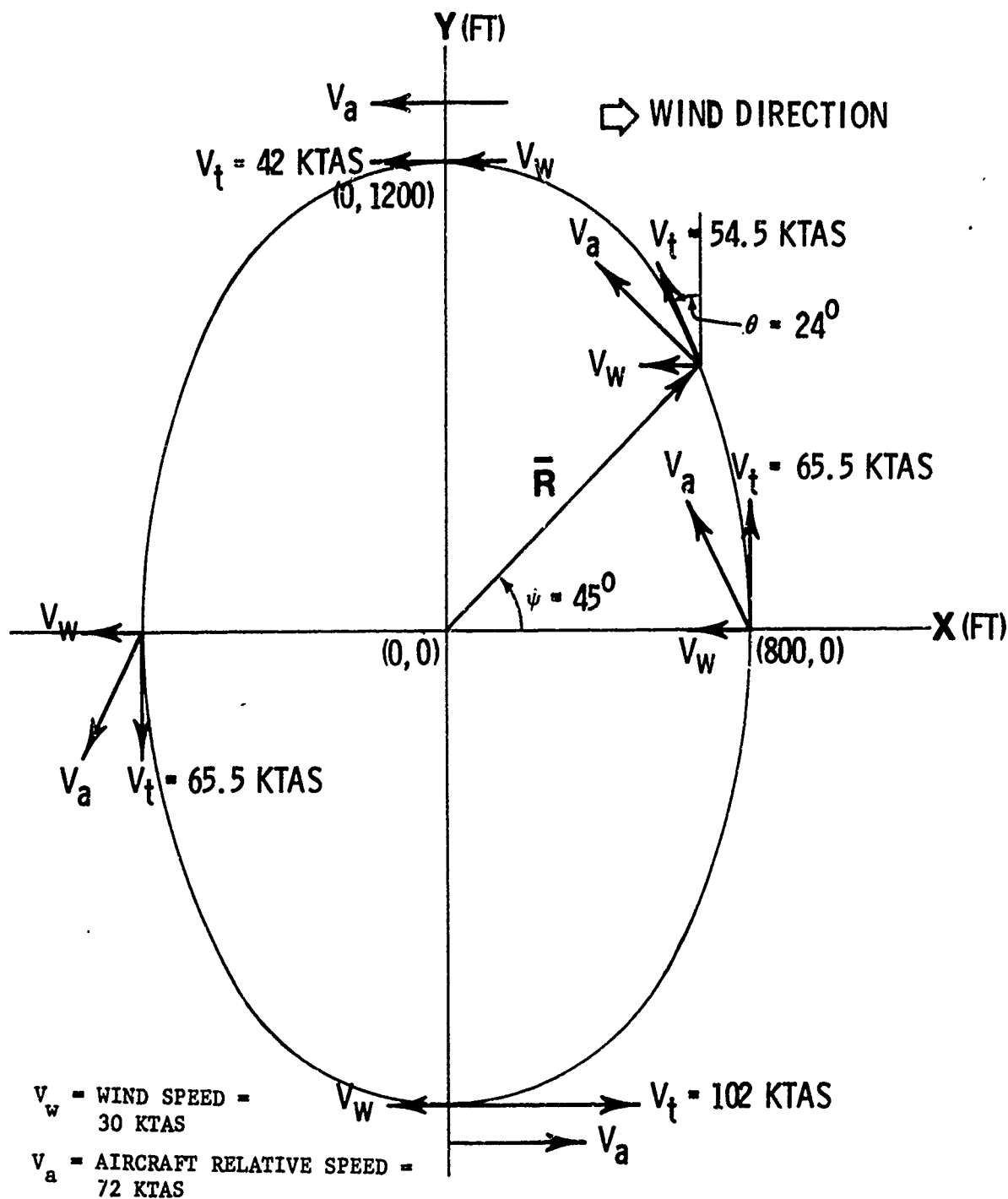R = AIRCRAFT POSITION VECTOR

FIGURE 3

AIRCRAFT ELLIPTICAL ORBIT

8

orbit transforms into a non-constant altitude orbit. Figure 4 shows a side view of two non-constant altitude orbits. In both orbits, the X and Y coordinates of the aircraft's position are found using the computer subroutine for a constant altitude circular orbit. The altitude of Orbit in Figure 4 is calculated from the expression:

$$Z = (X-X_{max}) \tan \ + Z_C$$

This simple elliptical orbit would be impossible to fly, since the vertical velocity of the aircraft is a very complicated function. However, this particular orbit is a good approximation of orbits that are possible to fly. Orbit 2 in Figure 4 is an orbit with a constant positive vertical velocity when flying in the direction of the prevailing wind and a constant negative vertical velocity when flying against the wind. It is more realistic to assume that the orbit with constant vertical velocities, i.e. Orbit 2, could be flown. Since both non-constant altitude orbits are very similar, the orbit that is simpler to model, i.e. Orbit 1, is utilized in the computer simulation.

2.3 Drogue Model

The drogue in the computer simulation is modeled by a sphere, as shown in Figure 1. The final mass point of the lumped mass model of the cable coincides with the center of the sphere. If the cable is assumed to attach to the center of the sphere, all the forces due to the final cable segment and due to the sphere will act through the center of gravity, and the three translational degrees of freedom of
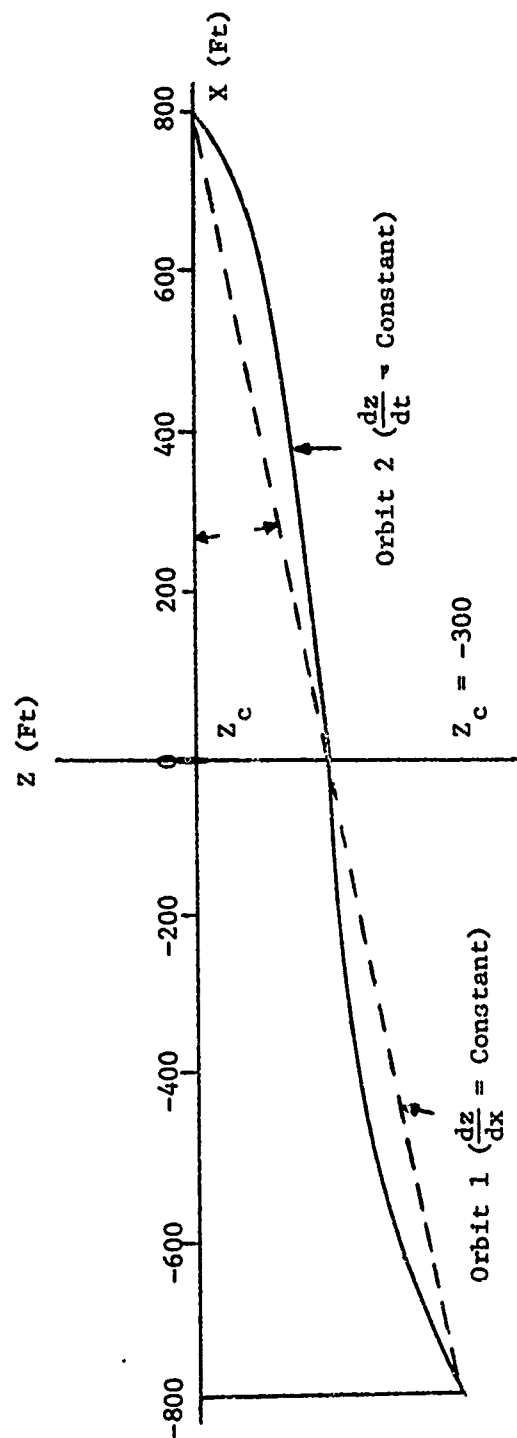
9

FIGURE 4

AIRCRAFT NON-CONSTANT ALTITUDE ORBITS

10

the final mass point will completely describe its motion. Thus, the lumped mass model is modified at the final mass point to include the weight, drag, and inertia force of the spherical drogue as forces acting on the final mass point.

An exact model of a drogue must include rotation. The cable cannot be attached at the center of a sphere with a finite radius, so the tension in the cable produces a moment about the center of gravity of the sphere. For a drogue with a more complex shape, the center of pressure will not coincide with the center of gravity, and aerodynamic forces will produce additional moments about the center of gravity. These moments produce rotation, and three additional equations of motion are necessary to describe the rotation.

The equations of rotational motion could be derived, but their addition would not significantly improve the analysis. During SNOWBIRD flight tests, a 25 lb conical drogue has been observed to fly with its axis always within 10° of the vertical in both a zero wind environment and a prevailing wind. A heavier drogue would have a greater amount of inertia and would align its vertical axis to within a few degrees of the vertical. Therefore, the drogue's rotational equations of motion are neglected in this analysis.

2.4 Determination of Number of Lumped Masses in Model

If there were an infinite number of mass points in the lumped mass model of the trailing wire and if the equations of motion could be solved by the computer with no round-off error, the motion of the

11

trailing wire would be described exactly by the coordinates of the lumped masses. However, since only a finite number of equations can be programmed on the computer, error in the model is inevitable. To complicate the situation, the time step used by the Runge-Kutta integration scheme must be very small to keep the integration from becoming unstable. Therefore, N, which is the number of lumped masses in the model of a cable, must be minimized to prevent excessive computer usage, but N must be large enough to reduce the error in the model to an acceptable level.

Computer tests indicate the optimum value of N. The computer program used for the tests calculates the steady state shape of the trailing wire in a zero wind environment (Hinnerichs/Crist, 1972). During the tests, the aircraft flies in a circular orbit. Since there is no prevailing wind, the cable's lumped masses and the drogue also fly in circular orbits. The drogue's orbit is specified and the program calculates the position of each mass point leading to the aircraft. The process cannot begin at the aircraft, since the tension in the cable at the aircraft is initially unknown. As the number of mass points in the lumped-mass model increases, modeling errors decrease. As N is increased, eventually it reaches a limiting value, above which a further increase in N results in only a minute reduction in modeling errors. Both physical dimensions of the aircraft orbit and cable tensions for an N greater than or equal to this limiting N are nominal values upon which to base errors. An acceptable N produces errors no larger than a few

12

per cent of the nominal values.

Tests were performed for each of the cable configurations analyzed in this paper. Table 1 tabulates modeling errors associated with different values of N for two cable configurations utilizing the SNOW-BIRD parameters described in Section 3. The errors are based on steady state shape calculations for the cables modeled by 200 lumped masses. For both cables with N equal to 10 the errors are too large, and with N equal to 20 the errors are acceptable. As N is increased beyond 20, modeling errors are not sufficiently reduced to justify the increase in computer time necessary to integrate the equations of motion. The tensions are always less for the 200 lumped mass model, so tensions in the 10 Cases of Section 4.2a are conservative. The progression angle is defined to be the angle between the aircraft and the drogue, with its vertex at the center of the aircraft orbit. The calculations in these tests take only a few seconds of central processor time on the Control Data Corp 6600 Computer.

A time step does not appear in the steady state shape program, as this program does not involve integration. Thus, the optimal N should be determined before attempting to find the optimal time step.

2.5 Determination of Time Step

The time step used by the Runge-Kutta integration scheme is called TSTEP. If TSTEP is too large, the integration will become unstable and the variables in the equations of motion will grow without bound. If TSTEP is too small, the integration will be stable, but valuable

13

Configuration	N	Aircraft Altitude (% error)	Radius of Aircraft Orbit (% error)	Progression Angle (% error)	Tension in Cable Segment of Aircraft (% error)	Tension in Cable Segment of Drogue (% error)
4,000 ft cable	10	.07	3.2	4.8	1.3	7.4
	20	.02	.2	1.5	.1	3.5
8,000 ft cable	10	1.72	10.1	10.8	34.9	15.0
	20	.28	2.3	2.4	3.6	7.1
	30	.06	.8	1.2	4.0	4.5
	40	.01	.4	.7	2.3	3.2

TABLE 1

MODELING ERRORS VERSUS N

computer time will be wasted and round-off errors could be significant.

The optimal TSTEP is found by choosing values for TSTEP and running the computer simulation. The cable is initialized in its steady state shape and flown in a zero wind environment. The drogue and the mass points should not move vertically if the integration is stable. The largest TSTEP for which the integration is stable is the best TSTEP. If TSTEP is marginally stable, the integration may not become unstable immediately. To insure that TSTEP is not marginally stable, a TSTEP smaller than the largest apparently stable TSTEP should be chosen. An initial guess at TSTEP should be small enough to integrate the highest frequency motion, which is the longitudinal vibration of the lumped masses. The initial guess is given by:

$$TSTEP = \frac{\tau}{10} = \frac{\pi}{5}\sqrt{\frac{m_i}{2 \times k_i}}$$

where: τ = period of vibration

m_i = mass of ith point

k_i = spring constant for segment i.

The Runge Kutta integration requires that TSTEP $\approx$ .016 sec for the model of the 8,000 ft SNOWBIRD cable consisting of 20 lumped masses. This is equivalent to .0008 sec/step/mass. Integrating with TSTEP = .0163 takes approximately 4.8 minutes of central processor time on a CDC 6600 Computer for each circular orbit flown in a zero wind environment. Since the actual flying time is about 20.5 sec/orbit, the ratio

15

of central processor time to aircraft flight time is approximately
14:1. In a prevailing wind, the flying time will increase slightly.
For example, in a 15 knots true air speed (KTAS) wind, flight time is
24.2 sec/orbit, and in a 30 KTAS wind, flight time is 30.4 sec/orbit.

SNOWBIRD PARAMETERS

The parameters to be varied for a complete parametric study of a
trailing wire system would include the size and shape of the aircraft
orbit, the relative velocity of the aircraft, the physical properties
of the cable, and the physical properties of the drogue. Each trailing
wire configuration would be flown under a variety of wind conditions.
The results of this paper constitute a limited parametric study of the
SNOWBIRD system, a trailing wire system flight tested by Air Force
Academy personnel.

3.1 Aircraft Orbits

The aircraft orbits used for the computer simulation of the
SNOWBIRD system are typical of the orbits flown by the U-10 during
SNOWBIRD testing. The aircraft velocity is 72 knots true air speed
(KTAS) relative to the wind for both circular and elliptical orbits.
For a circular orbit flown with a zero wind condition, this aircraft
velocity corresponds to the U-10 flying at a 30° bank angle with an
indicated speed of either 60 knots indicated air speed (KIAS) at an
altitude of 12,825 ft (4,000 ft cable) or 55 KIAS at an altitude of
16,900 ft (measured from sea level) (8,000 ft cable). The altitude of

16

the towing aircraft varies in order to maintain similar drogue altitudes
for different length cables. The radius of every circular orbit in the
simulation is 800 ft. The orbital parameters for a circular orbit
flown with a zero wind condition are calculated from the equations:

$$\dot{\phi} = \frac{g \tan \lambda}{V_t}$$

$$R = \frac{V_t}{\dot{\phi}}$$

where: $\dot{\phi}$ = angular velocity of aircraft

V_t = tangential or ground track velocity of aircraft

λ = bank angle of aircraft

R = radius of circular orbit

g = acceleration of gravity

(Liller, 1969)

If a prevailing wind exists, λ must continually be corrected in order
to fly a circular orbit and both V_t and $\dot{\phi}$ will vary; but the relative

aircraft velocity, the orbit altitude, and R are the same as in a zero
wind environment. All elliptical orbits in the simulation have a semi-
major axis of 1200 ft and a semi-minor axis of 800 ft.

The circular orbit in Figure 2 and the elliptical orbit in Figure
3 represent SNOWBIRD orbits.

3.2 Cable Properties

The following cable properties were measured for the SNOWBIRD
cable:

diameter = .048 in.

weight/unit length = .00500 lb/ft

modulus of elasticity = 10.2×10^6 lb/in^2.

Both 4,000 and 8,000 ft cable lengths (unstretched) are simulated on
the computer. Comparisons are made between steady state shapes of the
two lengths of cable under similar flight conditions.

Aerodynamic lift and drag coefficients of the cable are ex-
pressed in the forms: $C_L = 1.03 \sin^2\alpha \cos\alpha$

$$C_D = .022 + 1.03 \sin^2\alpha \sin\alpha$$

where: = angle of attack of cable segment.

Lift and drag forces are given by: $L = C_L qA$

$$D = C_D qA$$

where: A = planform area of cable segment (length x diameter)

q = dynamic pressure.

Lift and drag forces are located in a plane formed by the relative
fluid flow vector and the cable segment. (See Figure 5) The trans-
verse aerodynamic force is normal to this plane, and caused by circula-
tion around a stranded cable. Transverse aerodynamic forces are insig-
nificant and will be neglected in this analysis. This has been the
normal approach taken by former investigators of cable systems under
hydrodynamic loading. This analysis also neglects fluctuating forces
attributed to vortex shedding in the wake of the cable. These forces
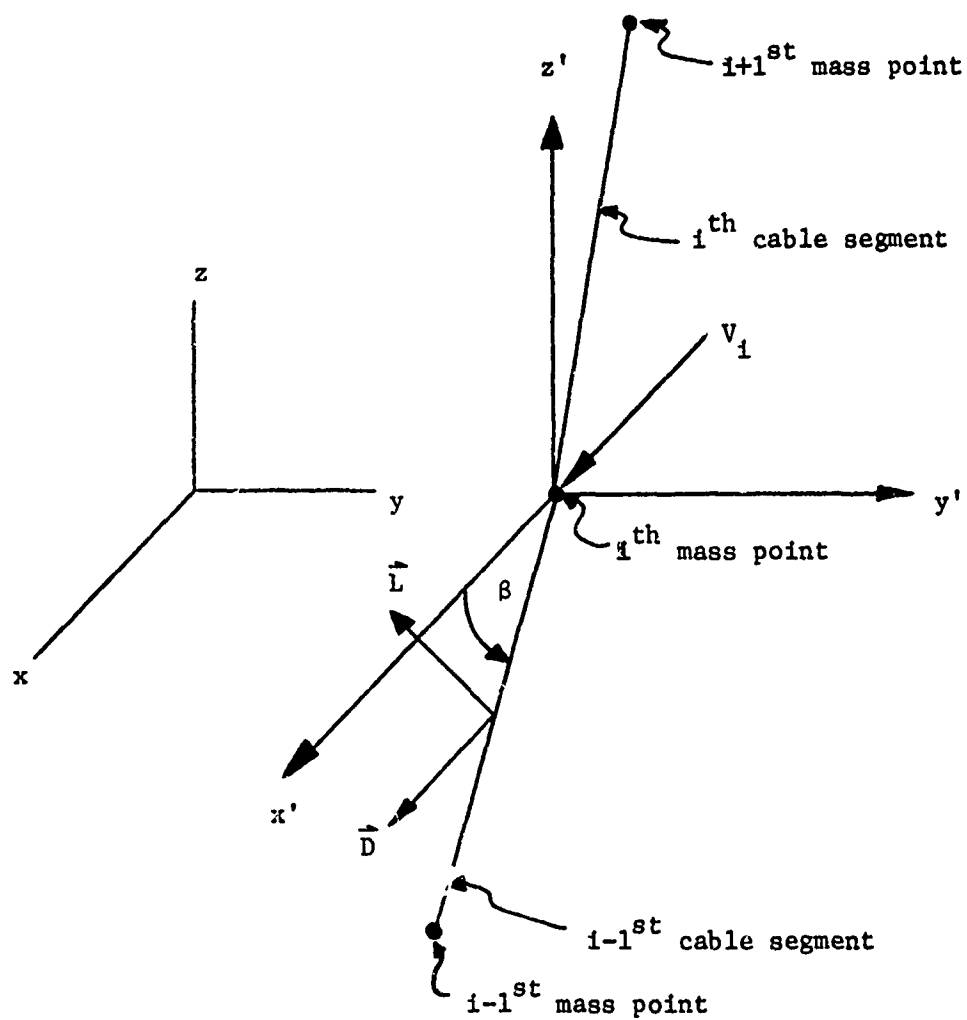could possibly result in flutter called "Transmission Line Gallop".

18

FIGURE 5

AERODYNAMIC FORCES ACTING ON CABLE

19

Vortex shedding has also been omitted from most studies of cable systems under hydrodynamic loading (Casarella and Parsons, 1970, p. 35).

3.3 Drogue Properties

The following properties were assumed for the spherical drogue: .

Radius = .42 ft.

Weight = 25 lb.

In one simulated flight test the drogue weight was increased to 100 lb while the radius remained constant.

Aerodynamic lift and drag coefficients for a spherical drogue are expressed in the form: $C_L = 0.$

$$C_D = .6 .$$

Lift and drag forces are given by: $L = 0.$

$$D = C_D qA$$

where: A = cross sectional area of sphere (π x radius^2).

The air density for all aerodynamic force calculations is taken from a curve fit of the NACA Standard Atmosphere Tables.

3.4 Wind Conditions

Two types of wind profiles were used in the computer analysis. The simplest and most frequently used is the constant wind profile. This profile is used when comparing dissimilar cable configurations. The constant wind profile assures the analyst that variations in the cable shapes and motions are not due to a change in shape of the wind profile, but instead are a consequence of differences in the physical

20

parameters of the cable configurations. The power law profile is used

to approximate the wind profile at low altitudes. The power law is

stated as:

$$V_2 + V_1 \left[\frac{h_2}{h_1} \right]^m$$

where: V_2 = wind speed at altitude h_2

V_1 = wind speed at altitude h_1

m = .35

(Liller, 1969, p. 38)

Since SNOWBIRD test flights were flown at a location where ground level

was 8,900 ft, in the computer simulation h_1 = 12,900 ft and h_2 ranges

from 8,900 ft to 12,900 ft. At altitudes greater than h_1, the wind

profile becomes a constant profile.

The wind speed for the computer simulation took on values of 0,

15, and 30 KTAS.

DISCUSSION OF RESULTS

4.1 Determination of Cable Lengths

Figure 6 is a plot of the radius of the drogue orbit for various

cable lengths flown in a zero wind environment. The aircraft orbit is

the same for each cable length, and is the same size as the circular

orbit in Figure 2. Since V_w is 0, both V_a and V_T are 72 KTAS. The

drogue altitude is 9,100 ft. The aircraft altitude ranges from 18,940

21

ft for a 10,000 ft cable to 9,420 ft for a 500 ft cable.

In order to study the effect that the cable length has upon the
motion of a trailing wire system in a prevailing wind, two lengths of
cable from Figure 6 were chosen to be flight tested. A 4,000 ft cable
was chosen, since for a shorter cable the drogue orbital radius is in-
tolerably large. An 8,000 ft cable was chosen, since increasing the
cable length beyond 8,000 ft does not significantly reduce the drogue
orbital radius.

4.2 Comparison of Flight Configurations

A computer simulation consisting of twelve different orbiting
trailing wire configurations has been arranged into ten representative
cases (Case 1-10) in a movie. (Trailing Wire Antenna Configurations
Using Snowbird Cable Towed by U-10 Aircraft) Individual frames of the
movie are presented in this report. Time exposures of each case follow
in the analysis.

4.2a Individual Frames

Five individual frames of Cases 1-10 appear in Figures 7a through
16e. For each case the sequence of frames labeled "a" through "e"
presents similar information. Figures 7-16a are title frames describing
the case and providing a legend in order to distinguish between differ-
ent cables. Figure 7-16b show three orthogonal projections of the
cables. The aircraft is located at the point on the orbit coincident
with the positive X axis. The cables appear to be smooth curves, but
they actually consist of 20 straight line segments. Figures 7-16c are

22
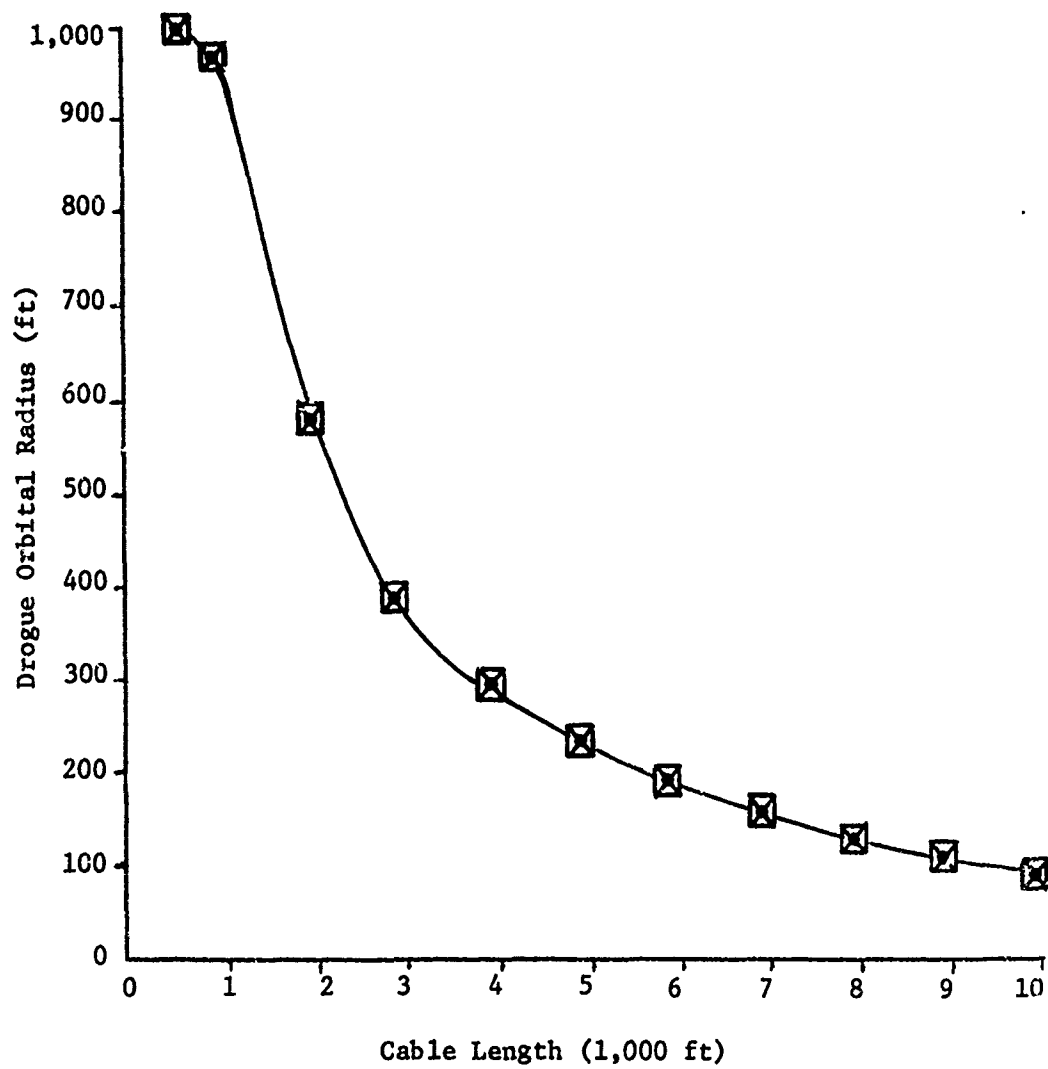
FIGURE 6

RADIUS OF DROGUE ORBIT VERSUS CABLE LENGTH

plan views, i.e., projections onto a horizontal plane, of the aircraft and drogue orbits. The aircraft and drogue fly counterclockwise in their orbits. Figure 7-16d are projections of the drogue orbit onto a vertical plane containing the X axis. These figures depict the vertical oscillation of the drogue, or the drogue yo-yo. Figures 7-16e plot the tensions in the cable segment attached to the aircraft. This segment is particularly interesting, since cable tensions are generally greatest at the aircraft. In Figures 7-16d and Figures 7-16e, the yo-yo and the tension are plotted for four identical orbits of the aircraft. The motion of the cable is identical for each cycle because the cable has been flying long enough to attain a steady state shape. Table 2 depicts a tabular summary of the information contained in Figures 7a through 16e.

Two suspended cables in the X-Z projections of Figures 9-12b present additional information for Cases 9-12. These suspended cables, being in equilibrium, are motionless. One cable is suspended from the center of the aircraft orbit, while the second cable hangs from the position on the orbit coincident with the positive X axis. The envelope for the motion of the towed cable consists of the area between the two suspended cables in the X-Z projection. The entire cable will not remain within the envelope during a complete aircraft orbit. Because the wind blows in the positive x direction, the uppermost section of the cable is located outside the envelope when the aircraft has a negative X coordinate, while the lowermost section of cable never leaves the envelope.

24

Case	Time(Sec) Cycle	Drogue Peak to Peak Yo-Yo (Ft)	Drogue Average Ascending Speed (ft/sec)	Drogue Average Descending Speed (ft/sec)	Peak Tension in Cable at Aircraft
1 (Blue)	41.0	0.	0.	0.	63.8
1 (Black)	41.0	0.	0.	0.	43.9
2 (Blue)	52.2	129.	9.0	10.8	69.9
2 (Black)	52.2	179.	13.2	14.5	48.7
3	47.9	1,247.	38.9	78.7	144.9
4	42.9	682.	26.3	40.1	89.1
5	53.4	736.	20.2	42.3	92.6
6	54.1	990.	32.0	42.7	78.8
7 (Blue)	Same as Case 4				
7 (Black)	42.9	608.	24.2	34.2	58.2
8 (Blue)	42.9	332.	13.0	19.1	163.1
8 (Black)	Same as Case 4				
9 (Blue)	42.9	338.	15.2	22.3	76.3
9 (Black)	Same as Case 4				
10 (Blue)	42.9	603.	23.3	36.4	86.2
10 (Black)	Same as Case 4				

TABLE 2

SUMMARY OF INFORMATION CONTAINED
IN FIGURES 7a-16e

25

CASE 1

This case illustrates the advantages of towing an 8,000 ft cable compared to a 4,000 ft cable when flying a circular orbit in a zero wind environment.

Figure 7b

The projections show that the 8,000 ft cable has much longer hanging chan the 4,000 ft cable, i.e., a straight line drawn from the aircraft to the drogue provides a better approximation to the shape of the 4,000 ft cable. The progression angles are 290° for the 8,000 ft cable and 195° for the 4,000 ft cable. Thus the 8,000 ft cable has more coiling and therefore more slack than the 4,000 ft cable.

Figure 7c

The plan view of the drogue orbit for both cables is a circle. If the aircraft flies in a circular orbit with no prevailing wind, every point on the cable will travel in a circular orbit.

Since the aircraft and the drogue both have the same angular velocity, the tangential velocity of the drogue will be less than the aircraft tangential velocity. The tangential velocities for this case are:

V_T aircraft = 122. ft/sec

V_T drogue for 8,000 ft cable = 21. ft/sec

V_T drogue for 4,000 ft cable = 46. ft/sec

Figure 7d

For an aircraft flying in a circular orbit in the absence of a prevailing wind, each point on the cable orbits at a constant altitude.

26

Therefore the drogue yo-yo is zero. (In this context the term yo-yo applies to the peak to peak displacement of the drogue's vertical oscillation.)

Figure 7e

The peak cable tensions are a few pounds less than the system dead weights for both the 8,000 ft and 4,000 ft cables. The dead weight of a trailing wire system consists of the weight of the cable and the weight of the drogue. The dead weight of the SNOWBIRD cable with a 25 lb drogue is 65 lb for the 8,000 ft cable, and 45 lb for the 4,000 ft cable.

Both the 8,000 ft and 4,000 ft systems in CASE 1 provide a platform that could be used for many practical applications. Tensions are not near the 300 lb breaking strength of the particular cable used. Both the tangential velocity and the drogue plan area are less for the 8,000 ft cable, so it would be easier to utilize.

Flight conditions have been idealized for this case, since there is no wind and the aircraft flies in a circular orbit. CASE 2 studies the same two cable systems; however, the aircraft flies in an elliptical orbit.

CASE 2

This case illustrates the advantages of towing an 8,000 ft cable compared to a 4,000 ft cable when flying an elliptical orbit in a zero wind environment.

27

Figure 8b

The projected views of this case are very similar to the projected views of CASE 1 (Figure 7b). The slack is again greater for the 8,000 ft cable.

Figure 8c

The plan view of the drogue orbit for both cable systems resembles an ellipse. The plan views of both the aircraft and drogue elliptical orbits circumscribe the corresponding plan views of the aircraft and drogue circular orbits of CASE 1 (Figure 7c). However, if the aircraft circular orbit circumscribed the aircraft elliptical orbit, the drogue circular orbit would circumscribe the drogue elliptical orbit.

Figure 8d

Since the aircraft orbit is not circular, the drogue oscillates vertically. The two crests in a complete cycle of the drogue's motion occur as the aircraft crosses the Y axis, and the two troughs per cycle occur as the aircraft crosses the X axis. As the aircraft flies counterclockwise around the orbit from the positive X axis to the positive Y axis, the slack in the cable decreases and the drogue rises. The more slack that exists in the system, the less the drogue will rise. Since there is more slack in the 8,000 ft cable than in the 4,000 ft cable, the yo-yo is less for the 8,000 ft cable.

Figure 8e

The peak tensions for both cable systems are less than 10% greater than their respective dead weights. Flying the system in a prevailing

28

wind will produce much greater tensions.

The 8,000 ft cable has better flight characteristics than the 4,000 ft cable when flying an elliptical orbit in a zero wind environment. Both the horizontal and vertical displacements and velocities are less for the 8,000 ft cable. Tensions in this case are so low that they are not critical in the design of either system.

Comparing CASE 1 with CASE 2, one concludes that in a zero wind condition, the aircraft should be flown in a circular orbit to obtain optimal flight characteristics of the drogue. Because the aircraft cannot be flown in a perfect orbit, the length of the cable is important. As the length of the cable increases, the yo-yo motion of the drogue decreases. This has been observed in SNOWBIRD flight tests.

CASE 3

This case demonstrates the detrimental effect that a 30 KTAS prevailing wind has upon the yo-yo of the drogue and the cable tensions for an 8,000 ft cable.

Figure 9b

In the X-Z projection the towed cable remains entirely within the envelope formed by the two suspended cables. The trailing 2,000 ft of the cable hangs nearly vertical.

Figure 9c

The plan view of the drogue orbit has a smaller area in this case than in CASE 1 (Figure 7c), where the aircraft flies in a similar circular orbit but with no prevailing wind. The drogue orbits downwind of

29

the aircraft at a distance slightly greater than one-half the cable length. Because the aircraft flies counterclockwise around the orbit and spends more time flying upwind than downwind, the drogue orbits on the positive Y side of the X axis.

Figure 9d

This much yo-yo could be very detrimental to the effectiveness of the trailing wire system. The average drogue velocity during descent, 78.7 ft/sec, makes it very difficult to land the drogue softl- in a 30 KTAS wind.

The highest altitude of the drogue occurs when the aircraft is furthest upwind, and its lowest altitude occurs when the aircraft is furthest downwind.

The yo-yo for the same system flown under the same wind condition but with V_t constant and equal to 72 KTAS is 1,300 ft.

Figure 9e

The peak tension is 123% greater than the dead weight of the system, and very near the 300 lb breaking strength of the SNOWBIRD cable.

As the aircraft flies upwind, the tension in the cable continually decreases. When the aircraft flies downwind, it doubles back on the cable and the drogue falls. Tensions in the cable decrease even further as the drogue falls. If the drogue were free-falling, its velocity would increase until it attained a terminal velocity of 289 ft/sec. Restraining tension in the cable causes the maximum drogue vertical velocity to be less than 100 ft/sec. Just prior to the aircraft

crossing the positive X axis, the drogue has pulled the cable taut, and a spike in the cable tension decelerates the drogue. A stress wave travels up the cable from the drogue to the aircraft. The velocity of the stress wave is $\sqrt{E/\rho}$ or 10,902 ft/sec. It takes 0.734 sec for the stress wave to travel up 8,000 ft of cable to the aircraft.

The yo-yo of the trailing wire system with a 25 lb drogue in a 30 KTAS wind would prohibit its use in many applications. Tensions are so very near the breaking strength of the SNOWBIRD cable that additional gust loading at the drogue could conceivably result in failure of the cable.

The 30 KTAS wind at a constant profile creates an extremely poor environment in which to operate the trailing wire system. Normally wind speeds will not be so high, since the system is flown near the ground. The power law profile (explained in the "Wind Conditions" section) used in CASE 10 gives a better approximation to the actual wind profile at altitudes within 4,000 ft of the ground, and the trailing wire system behaves better with a power law wind profile.

CASES 4-10 study methods used to reduce yo-yo and peak tensions when flying in a prevailing wind. The maximum wind speed for these cases is 15 KTAS.

CASE 4

This case demonstrates the detrimental effect that a 15 KTAS prevailing wind has upon the yo-yo of the drogue and the cable tensions for an 8,000 ft cable.

31

Figure 10b

In the X-Z projection the towed cable remains entirely within the
envelope formed by the two suspended cables. The trailing 4,000 ft of
the cable hangs nearly vertical.

Figure 10c

The plan view of the drogue orbit is even smaller in a 15 KTAS wind
than in the 30 KTAS wind (Figure 9c), and for all practical purposes,
the motion of the drogue is entirely vertical.

Figure 10d

Both the average descending velocity and yo-yo of the drogue are
approximately 50% of the corresponding values for a 30 KTAS wind (Figure
9d). It is still extremely difficult to land the drogue without its
crashing.

Figure 10e

The peak tension is only 37% greater than the dead weight of the
system, or less than one-half of the breaking strength of the cable.
The tensions are less than in a 30 KTAS wind (Figure 9e), since the
drogue descending velocity is less.

The average descending velocity and yo-yo of the drogue and the
peak tension in the cable caused by flying in a 15 KTAS wind are all
approximately 50% of the corresponding values for a 30 KTAS wind.

CASE 5

This case studies an 8,000 ft cable towed in an elliptical orbit
with the major axis of the ellipse perpendicular to the direction of

a 15 KTAS prevailing wind.

Figure 11b

The projections are nearly identical to the projections in CASE 4, where a circular orbit is flown under the same wind conditions (Figure 10b). In the X-Z projection the towed cable is entirely within the envelope formed by the two suspended cables.

Figure 11c

The plan view of the drogue orbit centers about the same location as the plan view in CASE 4 (Figure 10c). The area of the plan view here is only slightly greater than the area in CASE 4.

Figure 11d

The yo-yo is 7.9% greater than the yo-yo in CASE 4 (Figure 10d). However, since the path of the elliptical orbit is longer than the path of the circular orbit, the drogue average descending speed is only 5.5% greater in this case than in CASE 4. The drogue average ascending speed is less in this case than in CASE 4.

There are four distinct cycles of yo-yo motion. In CASE 2, where an identically shaped elliptical orbit is flown in a zero wind environment, there are eight cycles of yo-yo motion. Thus, the yo-yo for this case is primarily due not to the shape of the orbit, but to the length of time spent flying into the prevailing wind.

Figure 11e

The peak tension is only 2.5 lb greater than the peak tension in CASE 4 (Figure 10e).

33

The drogue flight characteristics and the cable tensions for this case are only slightly less desirable than those for CASE 4. From this case one concludes that irregularities in the shape of an orbit causing it to be noncircular will not limit the application of the trailing wire system, if the irregularities only increase the dimension of the orbit perpendicular to the prevailing wind by one-half the diameter of the desired circular orbit.

CASE 6

This case studies an 8,000 ft cable towed in an elliptical orbit with the major axis of the ellipse parallel to the direction of a 15 KTAS prevailing wind.

Figure 12b

Again the projections are nearly identical to the projections in CASE 4 (Figure 10b), and in the X-Z projection the towed cable is entirely within the envelope formed by the two suspended cables.

Figure 12c

The plan view of the drogue orbit is approximately 200 ft further downwind than the orbit in CASE 4 (Figure 10c). The area of the plan view is only slightly greater than the area in CASE 4.

Figure 12d

The yo-yo is 45.2% greater than the yo-yo in CASE 4 (Figure 10d). Since the path of the elliptical orbit is longer than the path of the circular orbit, the drogue average descending speed is only 6.5% greater in this case than in CASE 4.

As in CASE 5, there are four distinct cycles of yo-yo motion, and the yo-yo is primarily due not to the shape of the orbit, but to the length of time spent flying into the prevailing wind.

Figure 12e

The peak tension is 10.3 lb less than the peak tension in CASE 4 (Figure 10e).

The only factor making this case less desirable than CASE 4 is the increase in yo-yo. Since the drogue average descending speed is comparable to the speed in CASE 4, the drogue in this case would not be any more difficult to land than the drogue in CASE 4. The decrease in the peak tension in the cable is, of course, desirable.

From this case one concludes that irregularities in the shape of an orbit causing it to be noncircular, would limit the application of a trailing wire system only if yo-yo had to be kept to an absolute minimum. Significant irregularities are those that cause the dimension of the orbit parallel to the prevailing wind to be increased by one-half the diameter of the desired circular orbit.

CASES 4, 5 and 6 together infer that in a prevailing wind: 1) a circular orbit minimizes the yo-yo, average descending vertical velocity, and orbital plan area of the drogue; and 2) irregularities in the shape of the orbit, such that no dimension of the orbit is greater than one and one-half times the diameter of the desired circular orbit, will not limit the application of a trailing wire system. The analysis of time exposures of the cable motion will further conclude that the smallest

35

circular orbit is the most desirable.

CASE 7

This case compares an 8,000 ft cable with a 4,000 ft cable, when towed in identical circular orbits in a 15 KTAS prevailing wind.

Figure 13b

The cable projections are significantly different from those of CASE 1 (Figure 7b), in which the same cables are flown in a zero wind environment.

Figure 13c

The plan areas of the drogue orbits in this case are less than the areas in CASE 1 (Figure 7c). The area for the 8,000 ft cable is significantly less than for the 4,000 ft cable in both cases. Therefore, horizontal drogue velocities are significantly less for the 8,000 ft cable.

Figure 13d

The yo-yo for the 4,000 ft cable is 10.8% less than the yo-yo for the 8,000 ft cable. The drogue average descending velocity is 14.7% less for the 4,000 ft cable, so the drogue is slightly easier to land when flown on a 4,000 ft cable.

Figure 13e

For the 8,000 ft cable the peak tension is 37% greater than its system dead weight, and for the 4,000 ft cable the peak tension is 29.4% greater than its deadweight. The tension increases more for the 8,000 ft cable, since its drogue average descending velocity is greater.

36

The yo-yo and average descending velocity of the drogue and the peak cable tension are all less for the 4,000 ft cable, but the horizontal drogue motion is less for the 8,000 ft cable.

CASE 8

This case compares two trailing wire systems, both utilizing 8,000 ft cables and towed in identical circular orbits in a 15 KTAS prevailing wind. One system has a 25 lb drogue and the other a 100 lb drogue. Although the drogues are of different weights, they have the same dimensions.

Figure 14b

The cable with the 100 lb drogue hangs almost directly beneath the aircraft.

Figure 14c

The plan area of the drogue orbit is much larger for the cable with the 100 lb drogue. If the two systems were flown in still air, the drogue orbital radius would also be larger for the system with the heavier drogue. The plan area and location of the 100 lb drogue's orbit resemble the plan area and location of the 4,000 ft cable with a 25 lb drogue in CASE 7 (Figure 13c). Therefore, both shortening the cable and increasing the weight of the drogue increase the size of the plan view of the drogue orbit.

Figure 14d

The yo-yo of the 100 lb drogue is 51.3% less than the yo-yo of the 25 lb drogue, and its average descending velocity is 52.4% less than

for the 25 lb drogue.

Figure 14e

The peak tension in the cable with the 100 lb drogue is 23 lb greater than its system dead weight, while in the cable with the 25 lb drogue, the peak tension is 24.1 lb greater than its system dead weight. The increase in tension above the dead weight is nearly the same, because for the heavier system, the smaller drogue descending velocities are counteracted by the larger mass of the drogue. The peak tension for the system incorporating the 100 lb drogue is dangerously near the cable's 300 lb breaking point.

The yo-yo and average descending velocity of the drogue are less for the system with the 100 lb drogue. The peak cable tension and horizontal drogue motion are less for the system with the 25 lb drogue.

CASE 9

This case compares two identical 8,000 ft trailing wire systems flown in a 15 KTAS wind. One is towed in a constant altitude circular orbit, and the other in the nonconstant altitude orbit labeled "Orbit 1" in Figure 4.

Figure 15b

The projections of the two systems are very similar.

Figure 15c

The plan views of the drogue orbits are also nearly identical.

Figure 15d

The yo-yo and drogue average descending velocity of the system

employing a nonconstant altitude orbit are 43.1% and 44.4% less than the corresponding values for the system with a constant altitude orbit.

The difference in altitude between the highest and lowest points in the nonconstant altitude orbit amounts to 300 ft. The yo-yo for this orbit is 294 ft less than for the constant altitude orbit. Analysis of Section 4.2b "Time Exposures" will explain why this is such an excellent method of reducing yo-yo.

Figure 15e

The peak cable tension is 14.4% less for the nonconstant altitude orbit, because the drogue descending velocities are less.

The yo-yo and average descending velocity of the drogue and the peak cable tension are all less for the system flown in a nonconstant altitude orbit. The horizontal motion remains approximately the same for both systems. Of the methods studied in this report, flying in a nonconstant altitude aircraft orbit is optimal.

CASE 10

This case compares two 8,000 ft trailing wire systems flown in identical circular orbits with a 15 KTAS wind at the aircraft's orbit. For one system the wind profile is constant and for the other a power law wind profile is in effect.

Figure 16b

The cable loaded by the wind in a power law profile is exposed to lower wind velocities than the cable loaded by the wind in a constant profile as explained in Section 3.4; hence, it is not blown as far downwind.

Figure 16c

The reduced wind velocities result in a larger plan area of the drogue orbit.

Figure 16d

The yo-yo and drogue average descending velocity are less by 11.6% and 9.3% respectively for the system incorporating the power law wind profile.

Figure 16e

The peak cable tension is reduced by 3.3% when the power law wind profile is assumed.

It has been reported that the wind acting on the lower section of the cable influences the motion of the drogue to a greater extent than the wind on the upper section of the cable. (Liller, 1969, p. 59) The reduced wind velocities attributed to the power law profile occur near the ground and affect the lower section of the cable. When the power law wind profile is used, the vertical motion is reduced by roughly 10% in a 15 KTAS wind. Assuming that the reduction remains 10% for a 30 KTAS wind, the reduced vertical motion derived from Case 3 would still be very undesirable.

4.2b Time Exposures

Time exposures of Cases 1-9 appear in Figures 18-26. The exposures show the three orthogonal projections that appear in the computer simulated movie.

CASE 1

Figure 18 depicts surfaces swept out by the cables when there is no wind. The funnel shaped surfaces are symmetric about the X axis. Both surfaces attain their smallest cross-sectional diameter above the lower end of the cable and flare outward beneath this point due to the centrifugal force of the drogue.

CASE 2

The surfaces in Figure 19 are also funnel-shaped. In this case cross sections of the surfaces in the X-Y plane are ellipses and not circles as in Case 1.

CASE 3

The X-Z projection of Figure 20 shows that in a 30 KTAS wind the lowest 5,500 ft of cable remain within the envelope formed by the suspended cables during an entire orbit. There is no flare at the bottom of the surface. Thus the plan area of the drogue orbit is smaller if the trailing wire system is flown in a prevailing wind, than if it is flown in a zero wind condition.

Examination of the towed cable's motion with respect to the envelope formed by the suspended cables suggests a method of calculating the yo-yo and the average descending and ascending speeds of the drogue without having to integrate the dynamic equations of motion. The lowest section of cable moves in a path almost parallel to the suspended cables. When the aircraft flies upwind, the cable travels up the path, and as the aircraft flies downwind, the cable travels back down a nearly identical

path. This phenomenon occurs because the lumped mass model of the cable is perfectly flexible, i.e., the cable can support no bending moment. In actuality the cable can support only a negligible bending moment, so the model is a very good approximation. The uppermost section of the cable sweeps out a funnel shaped surface as the plane orbits, thus this section of the cable does not remain parallel to the suspended cables. If the junction between the uppermost and lowermost sections of the cable was located on the Z axis, there would be no yo-yo motion of the drogue. Since the junction is downwind of the Z axis, the distance from the aircraft to the junction is greater when the aircraft has a negative X coordinate than when the aircraft has a positive X coordinate. An approximation to the drogue yo-yo is the difference between the longest and the shortest straight line distances from the aircraft to the junction measured in the X-Z projection. The longest distance occurs when the aircraft is located at the position on its orbit coincident with the negative X axis, and the shortest distance occurs when the aircraft is positioned at the positive X axis. Applying this approximate method of determining the drogue yo-yo, it is difficult to locate the junction separating the uppermost and lowermost sections of the cable without first viewing a time exposure of the dynamic motion of the cable. Of course, the junction must be within the envelope formed by the suspended cables. It is sufficient to assume that the junction is located on a curved line parallel to, and midway between the suspended cables. Now the determination of the yo-yo is reduced to positioning the junction

42

on the curved line. Figure 17 is a graphical representation of the approximate method. Based on the experience gained from the time exposure observations a good approximation of the junction point is somewhere between a quarter and a half way down the suspended cable shape. The cable shape inferred here is the dashed line which is the computer predicted suspended cable shape based on the parameters listed on page 52. On Figure 17, point C was used for the yo-yo calculation. To indicate the freedom involved in positioning, the junction point on the suspended cable shape, points C' and C" were also used which resulted in less than 3% variation. In order to calculate the drogue's average descending and ascending speeds, one divides the yo-yo by the length of time the aircraft takes to fly the upwind and downwind portions of the orbit. By programming the aircraft to orbit with the velocities found in Section 2.2, these lengths of time are easily determined. In applying this approximate method to ascertain the yo-yo and average speeds of the drogue, all necessary calculations can be made on a programmable desk calculator, since finding the shape of the suspended cables involves static equations of equilibrium and is trivial compared to the integration of the dynamic equations.

Returning to Figure 20 and using the approximate method described above, the drogue yo-yo is calculated as 1,080 ft when the critical junction is located 1,600 ft, or one-fifth of the entire cable length from the orbit. This distance is measured along the curved line parallel to, and midway between the two suspended cables. The 1,600 ft

43
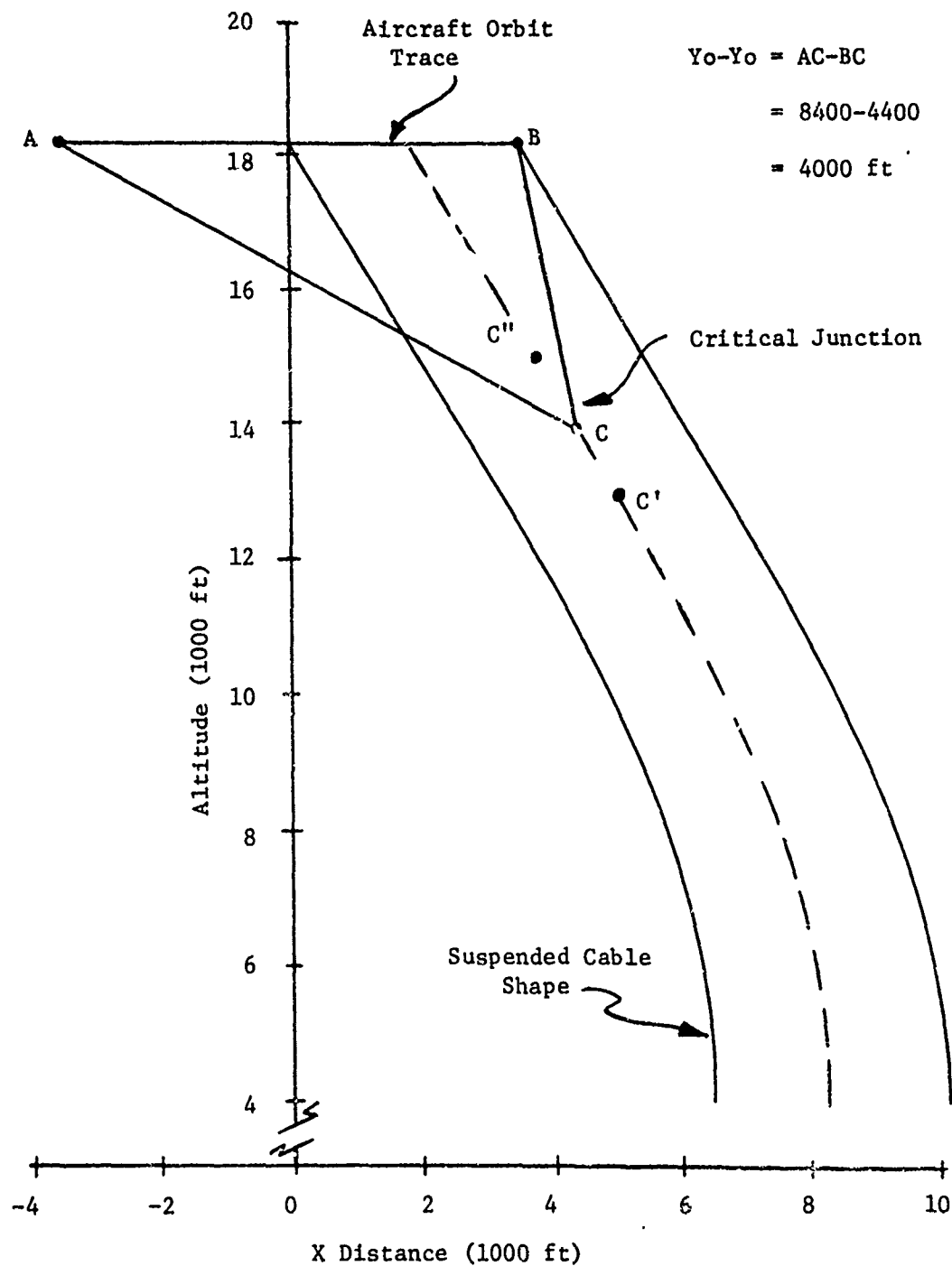
FIGURE 17

GRAPHICAL REPRESENTATION OF THE APPROXIMATE METHOD
FOR DETERMINING YO-YO

44

d'stance is selected since it gives accurate values of yo-yo for each of CASES 3-6. Using this value, the junction appears to be within the uppermost section of the cable. The yo-yo calculated by integrating the equations of motion for the system is 1,247 ft. The approximate value of yo-yo is 13.6% less than the exact value.

CASE 4

Applying the approximate method to Figure 21, the yo-yo turns out to be 680 ft when there are 1,600 ft separating the critical junction from the aircraft orbit. The exact yo-yo is 682 ft, so the approximate yo-yo is .3% less than the exact value.

Note in Figure 21 that there is no flaring at the bottom of the funnel-shaped surface in a 15 KTAS wind.

CASE 5

The same approximate method is used to find the yo-yo when flying an elliptical orbit. Since the X-Z projections of both the orbit and the envelope seen in Figure 22 are the same as in Figure 21 of CASE 4, then 680 ft of yo-yo will again be calculated when 1,600 ft of cable sepirate the aircraft orbit from the critical junction. This is 7.6% less than the exact value of 736 ft.

CASE 6

For the elliptical orbit in Figure 23, the approximate method predicts 1,000 ft of yo-yo when 1,600 ft of cable separate the aircraft from the critical junction. This is 1.8% greater than the exact value of yo-yo which is 990 ft.

CASE 7

In Figure 24 there is noticeable flaring at the bottom of the
surface swept out by the 4,000 ft cable, but no flaring at the bottom
of the surface generated by the 8,000 ft cable. Further analysis of
these surfaces in connection with the approximate method of determining
yo-yo explains why the yo-yo is nearly the same for both systems. The
vertical separation between the aircraft orbit and the critical junction
is greater for the 8,000 ft cable. If the junction had the same X
coordinate for both cables, the yo-yo would be less for the 8,000 ft
cable. However, the 4,000 ft cable is not blown as far downwind, and
its yo-yo is slightly less.

CASE 8

Increasing the weight of the drogue from 25 to 100 lbs causes the
flaring at the bottom of the surface to become appreciable, as seen in
Figure 25. The approximate method of determining yo-yo explains why
the heavier system has the least amount of yo-yo. The vertical separa-
tion between the aircraft orbit and the critical junction is greater
for the system employing a 100 lb drogue. This would cause the yo-yo
to be less for the heavier system, if the junctions had the same X co-
ordinate. Since the heavier system does not blow as far downwind, the
yo-yo is even further reduced.

CASE 9

In Figure 26 the surface generated by the 8,000 ft cable towed in
a nonconstant altitude orbit is most difficult to distinguish from the

surface generated by the cable towed in a constant altitude orbit.
The approximate method of determining the yo-yo explains why flying a
nonconstant altitude orbit it so successful in reducing yo-yo. Because
the two surfaces in Figure 26 are so much alike, the junction between
the uppermost and lowermost sections of cable is located at nearly the
same point for both surfaces. The vertical separation between the
junction and the aircraft as the aircraft is crossing the negative X
axis, is less for the nonconstant altitude orbit by approximately the
vertical distance between the highest and lowest points on the orbit.
Therefore, the yo-yo is reduced by nearly the entire altitude change
in the aircraft orbit.

One concludes after examining CASE 9 that the proper use of a high
speed cable reel is an effective means of reducing drogue yo-yo. The
yo-yo would be reduced by almost the entire length of cable that could
be reeled out as the aircraft orbited upwind and reeled in as the air-
craft orbited downwind.

The approximate method of calculating the drogue yo-yo by solving
the equations of static equilibrium works for other systems besides the
SNOWBIRD System. Air Force Academy personnel plan to flight test an
orbiting trailing wire system using a T-29 as the towing aircraft.
Parameters describing this system follow:

$$R = 3,190 \text{ ft}$$

$$V_t \,\widetilde{}\, 145 \text{ KTAS}$$

$$V_w = 30 \text{ KTAS}$$

47

h = 18,400 ft

Cable density = 234.7 lb/ft^3

Cable diameter = .17 in

Cable elastic modulus = 10x10^6 lb/in^2

Cable length = 16,000 ft

Drogue weight = 250 lb

Drogue radius (spherical) = 2.5 ft

The yo-yo calculated by integrating the equations of motion with N=20

equals 3,825 ft. Figure 17 graphically demonstrates the utilization

of the approximate method. The resulting yo-yo is 4,000 ft, or 4.4%

greater than the exact value of yo-yo. This system has pointed out the

versatility of the approximate method of calculating the drogue yo-yo.

It can be applied with adequate accuracy to almost any orbital trailing

wire system.

The surfaces generated by the towed cables flown in prevailing

winds, as seen in Figures 20-26, illustrate the inaccuracy of a simple

model of the orbiting trailing wire system that was proposed in the

University of Dayton Research Institute Technical Report UDRI-TR-70-31

of July 1970. The model is described in the Technical Report as

follows:

> "The model consists of assuming that centers of the
> circles made by each segment of the cable assume a
> shape similar to that of a motionless cable suspended
> from the center of the aircraft orbit. The surface
> in which the cable moves is then constructed around
> this line."
>
> (Crouch, Bauer, Kahle, 1970, p. 28)

48

This model adequately describes the motion of the uppermost section of the cable, but the lowermost section travels not around, but up and down a path nearly parallel to the suspended cable.

CONCLUSIONS

a. A lumped mass model of trailing wires can adequately predict the dynamics with a relatively few mass points and with a reasonable expenditure of computer time.

b. Both cross winds and orbital perturbations can cause the yo-yo phenomenon in cables.

c. In general, long cables towed from nonconstant altitude circular orbits from slowly flying, steeply banked aircraft with moderate weight drogues will give the most desirable cable characteristics.

d. Static analysis of Figure 17 adequately predicts the amount of yo-yo that will occur.

CASE 1

CIRCULAR FLIGHT PATH

NO WIND

Figure 7a

8,000 FT TOWED CABLE ——————

4,000 FT TOWED CABLE ——————

Figure 7b

51
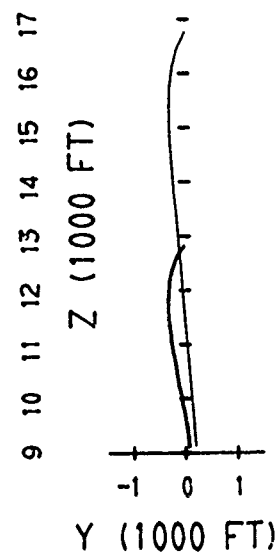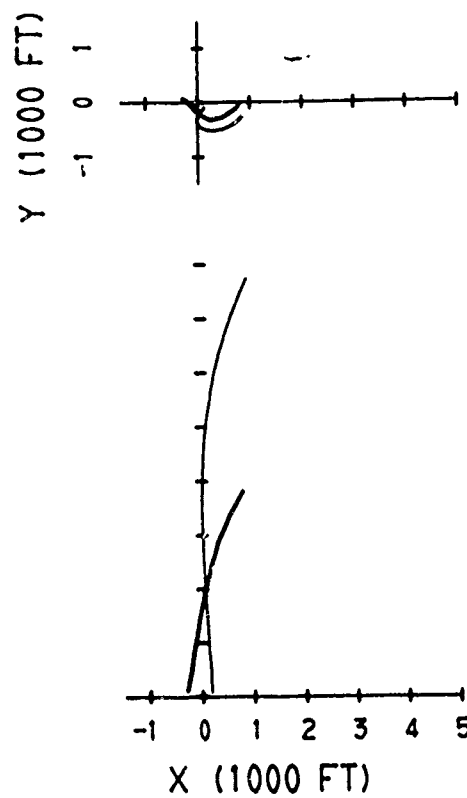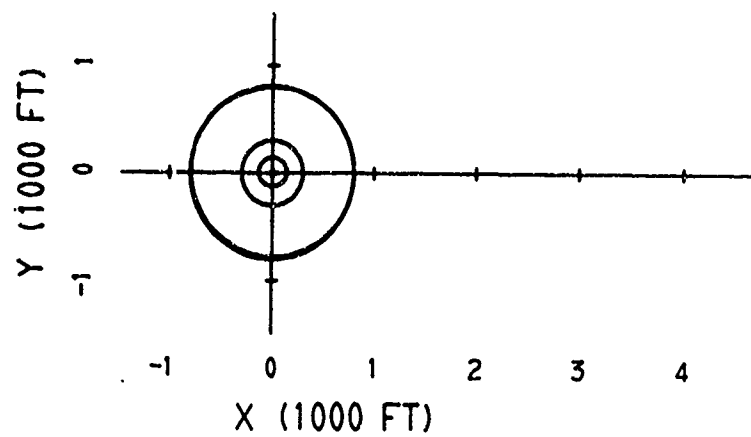
Figure 7c

Figure 7d

Figure 7e

52
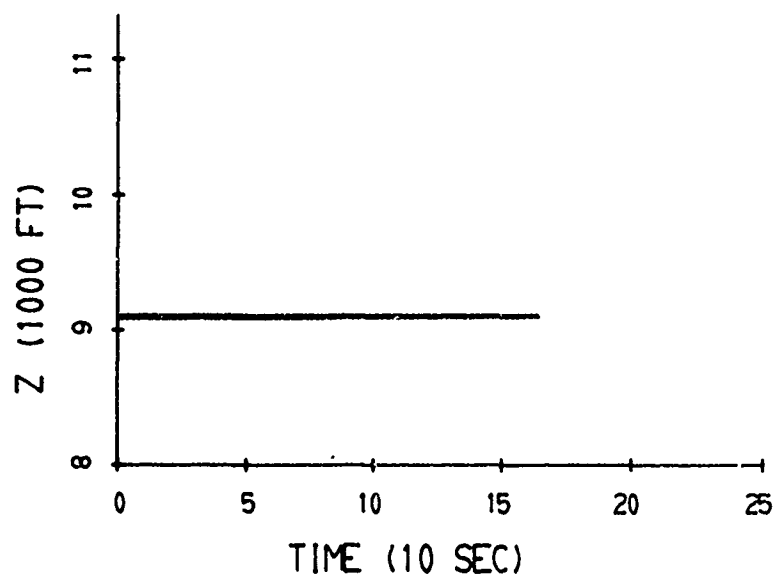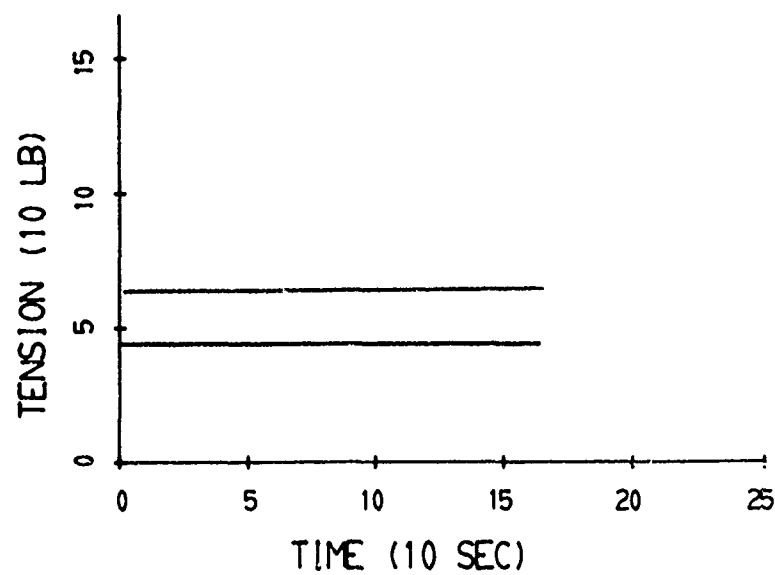
CASE 2

ELLIPTICAL FLIGHT PATH

NO WIND

Figure 8a

8,000 FT TOWED CABLE
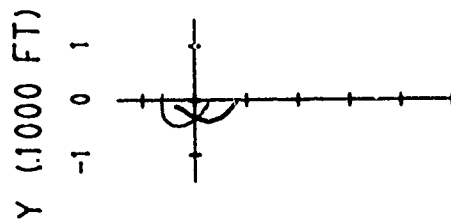
4,000 FT TOWED CABLE

Fibure 8b
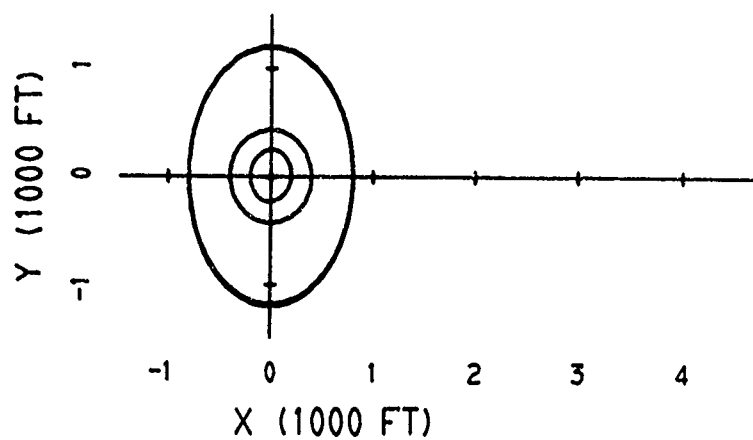
Figure 8c

Figure 8d

Figure 8e

54
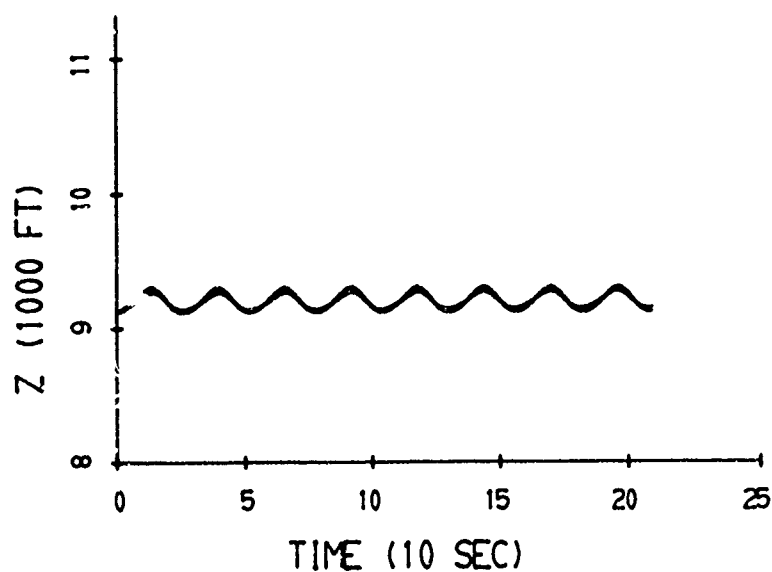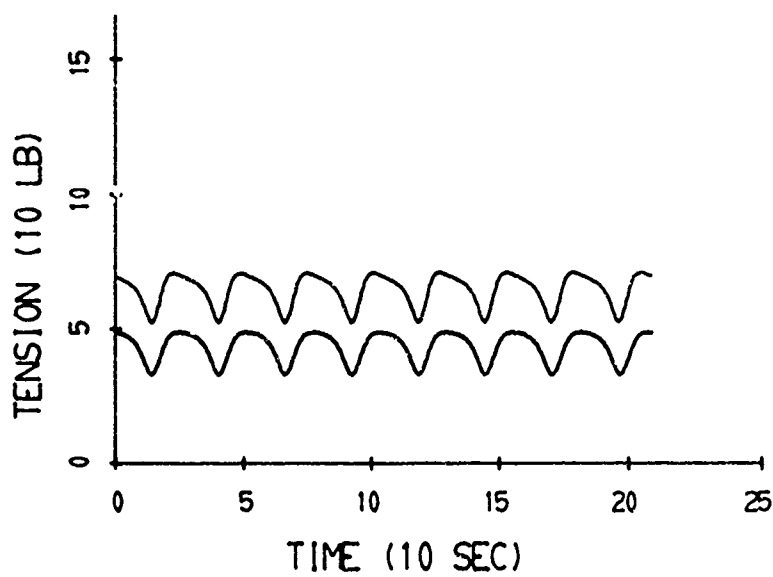
CASE 3

CIRCULAR FLIGHT PATH

30 KTAS CONSTANT WIND VELOCITY PROFILE

8,000 FT TOWED CABLE ——————

8,000 FT SUSPENDED CABLE ——————

Figure 9b

55
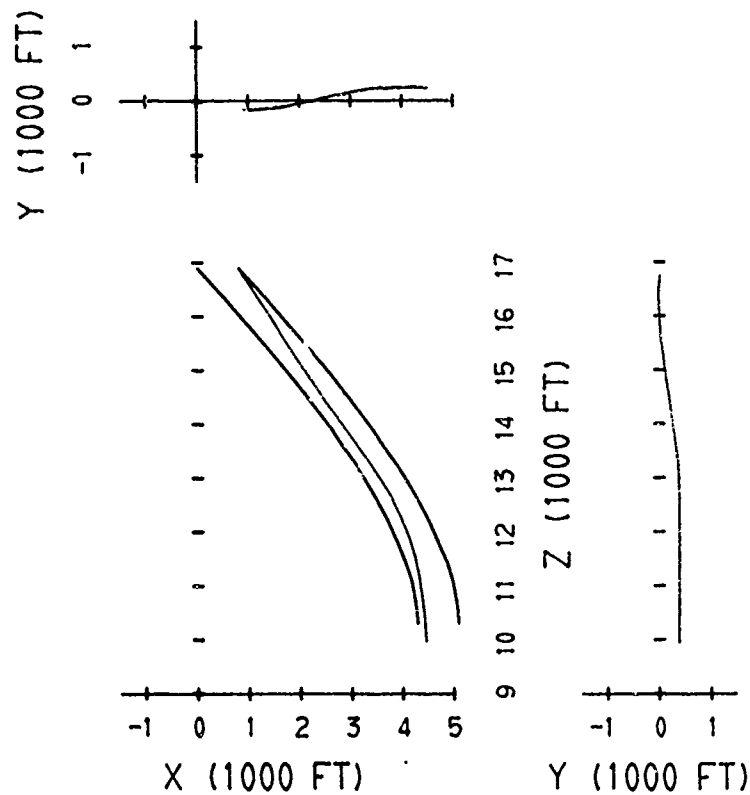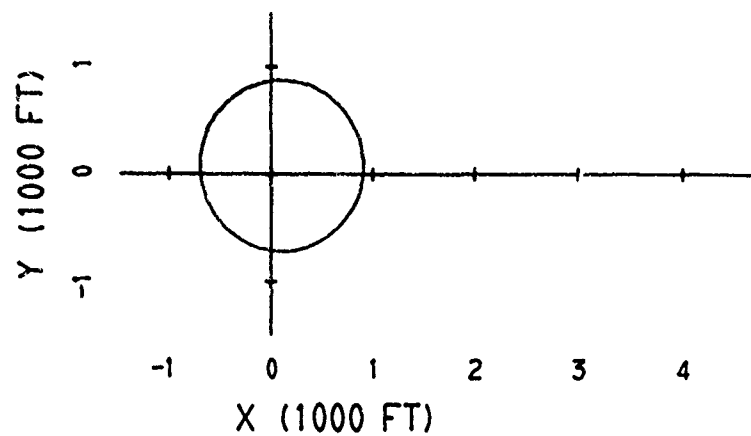
Figure 9c

Figure 9d

Figure 9e

56
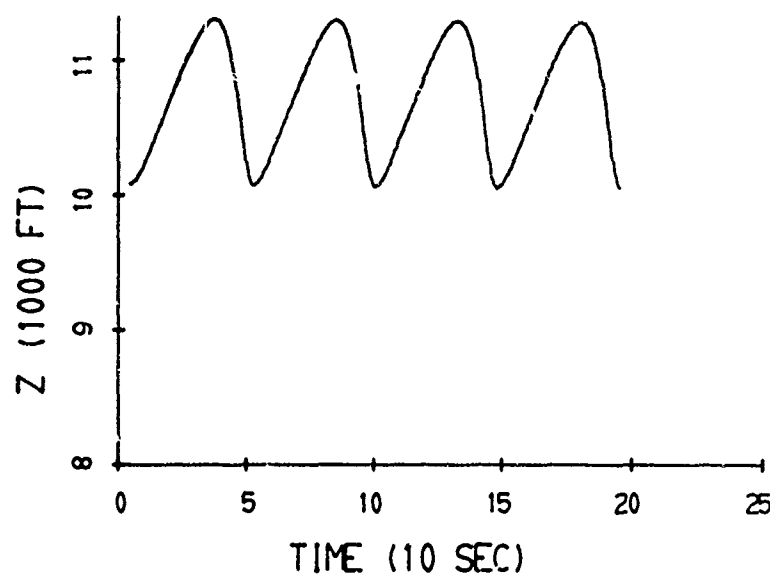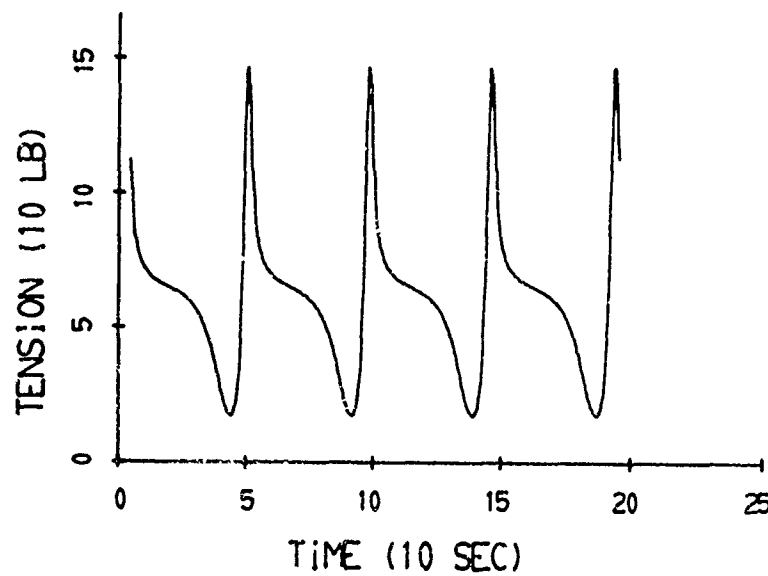
CASE 4

CIRCULAR FLIGHT PATH

15 KTAS CONSTANT WIND VELOCITY PROFILE   Figure 10a

8,000 FT TOWED CABLE   ———————

8,000 FT SUSPENDED CABLE   ——————

Figure 10b

57
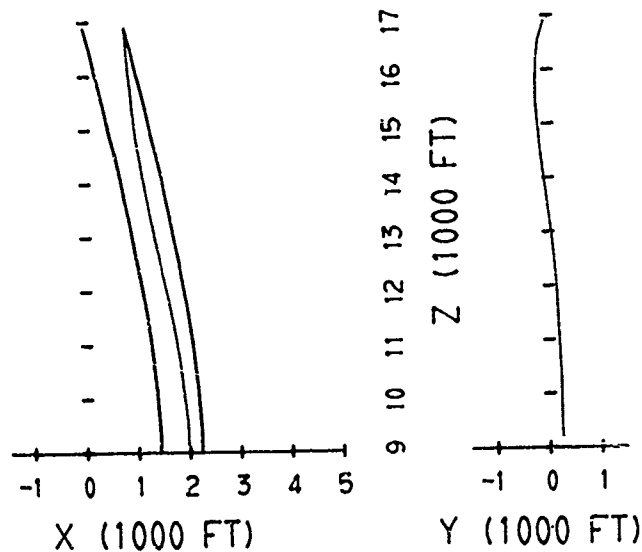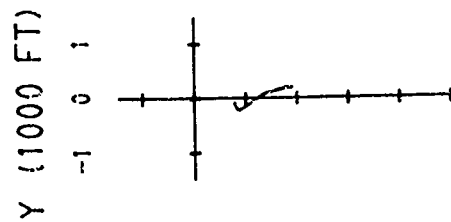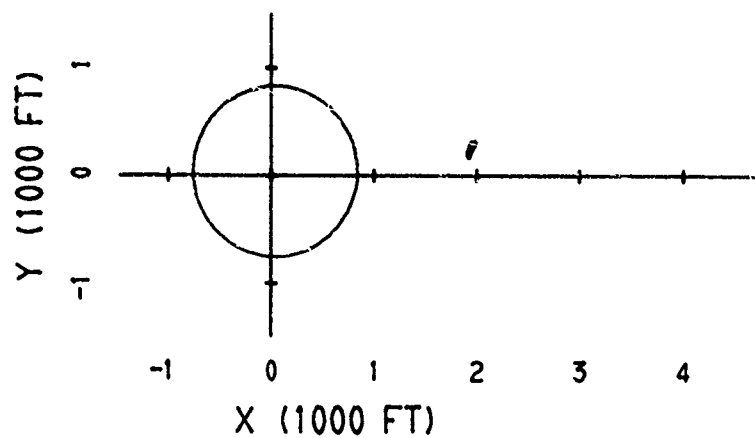
Figure 10c

Figure 10d

Figure 10e

58
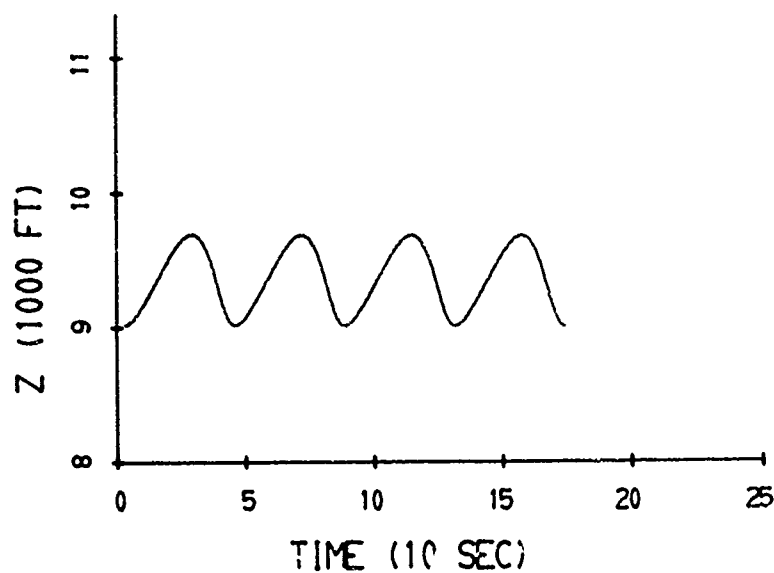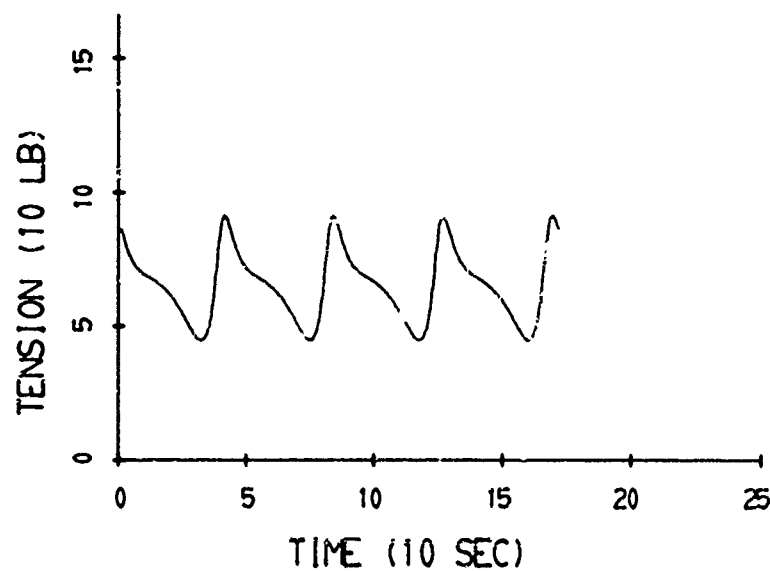
CASE 5

ELLIPTICAL FLIGHT PATH

15 KTAS CONSTANT WIND VELOCITY PROFILE

Figure 11a

8,000 FT TOWED CABLE ————————

8,000 FT SUSPENDED CABLE ————————
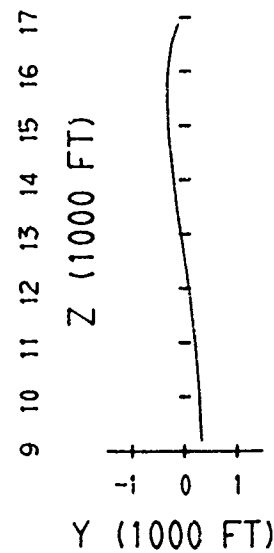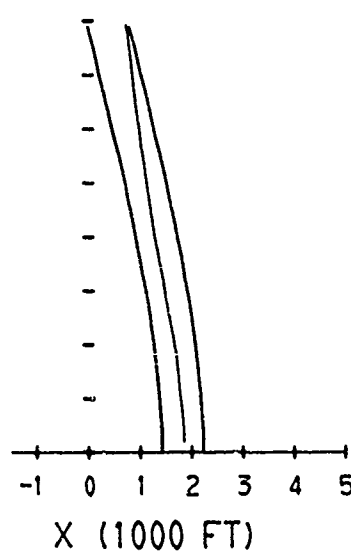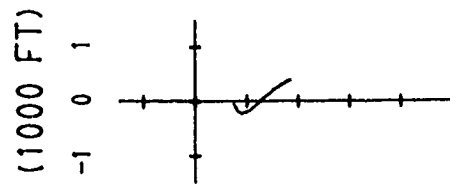
Figure 11b

Figure 11c
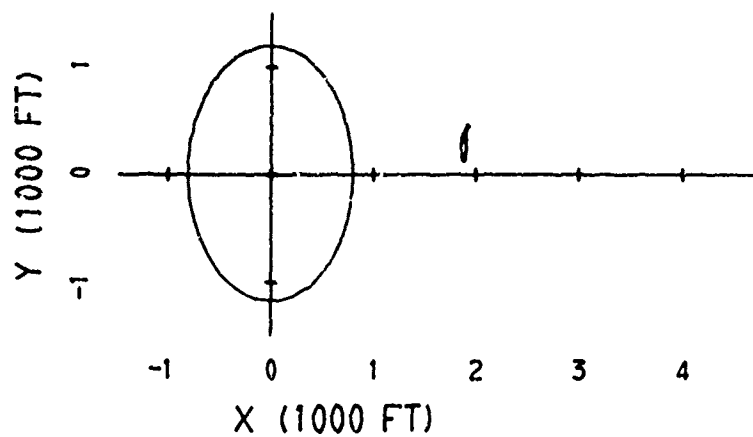
Figure 11d

Figure 11e

60
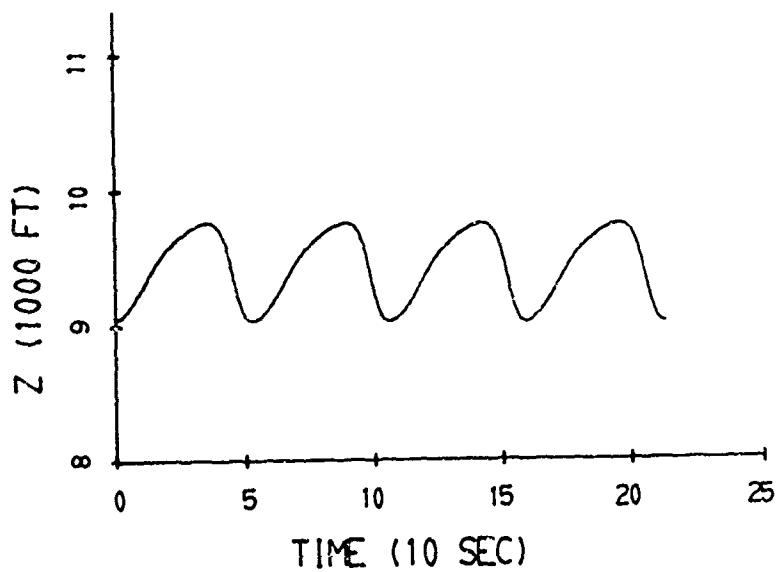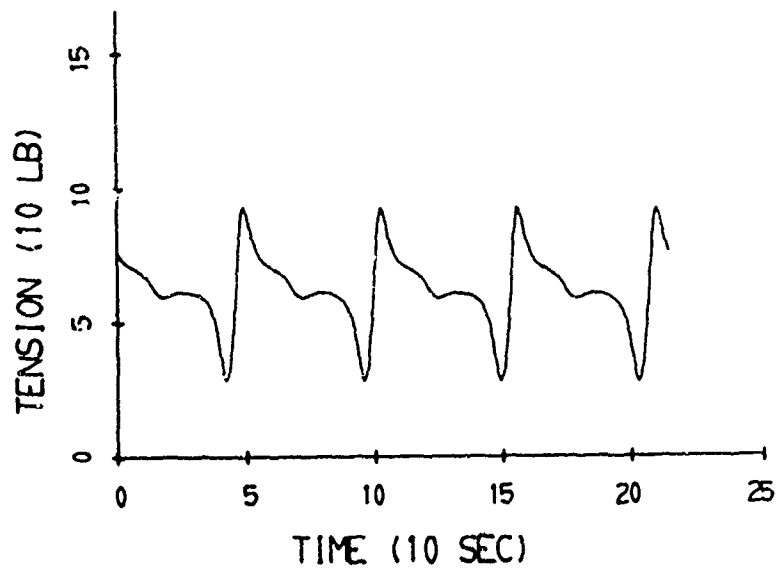
CASE 6

ELLIPTICAL FLIGHT PATH

15 KTAS CONSTANT WIND VELOCITY PROFILE
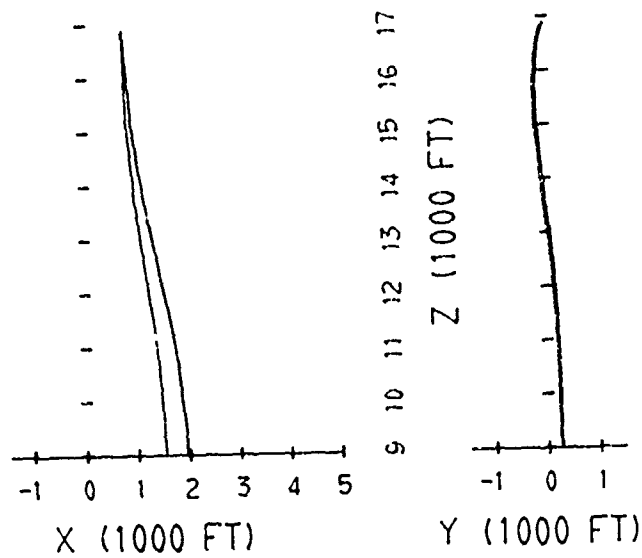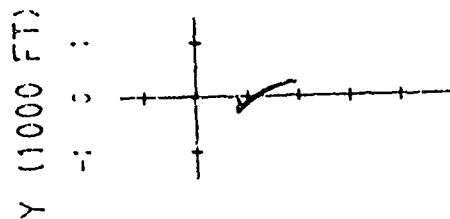
Figure 12a

8,000 FT TOWED CABLE ——————————

8,000 FT SUSPENDED CABLE ——————————
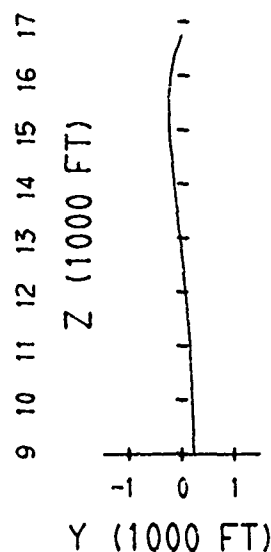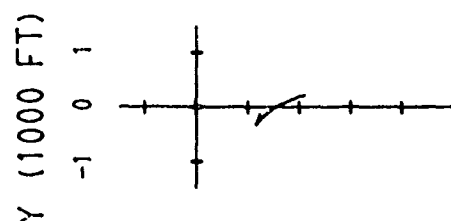
Figure 12b

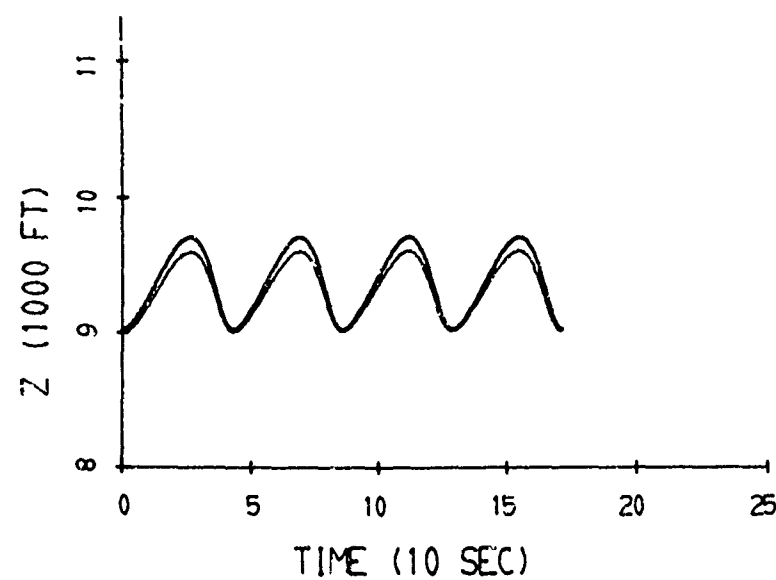Figure 12c
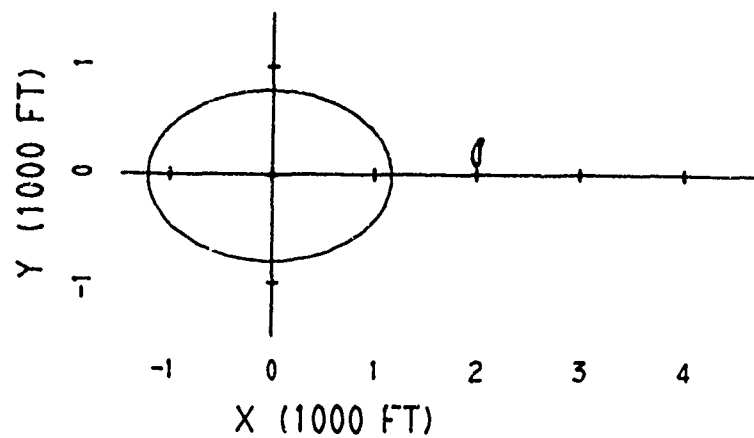
Figure 12d
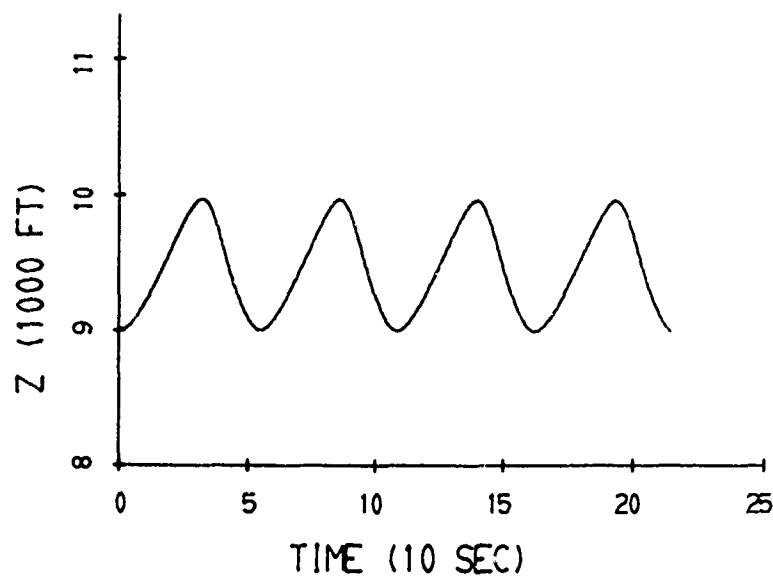
Figure 12~
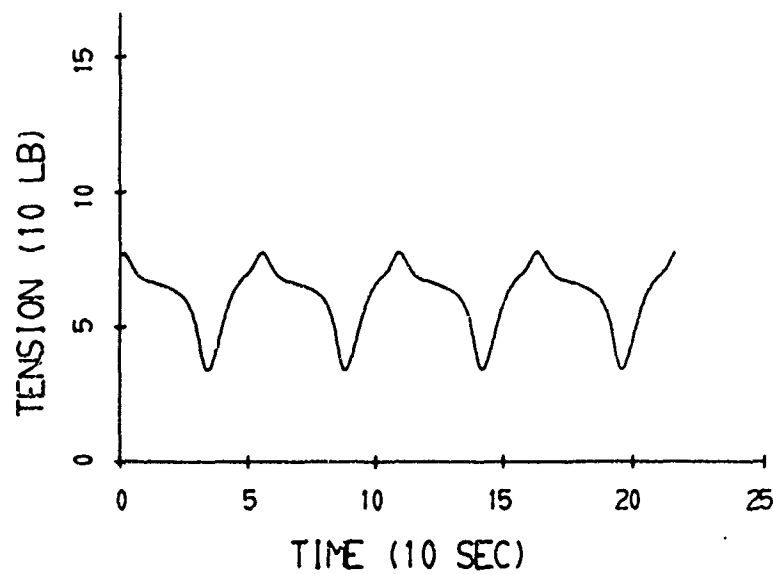
CASE 7

CIRCULAR FLIGHT PATH

Figure 13a

15 KTAS CONSTANT WIND VELOCITY PROFILE

8,000 FT TOWED CABLE ———————
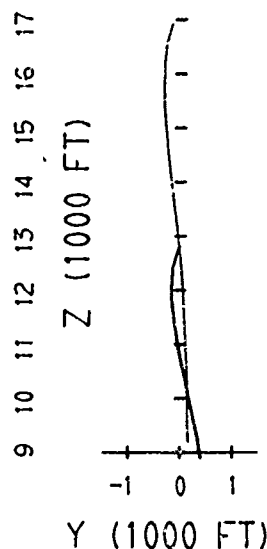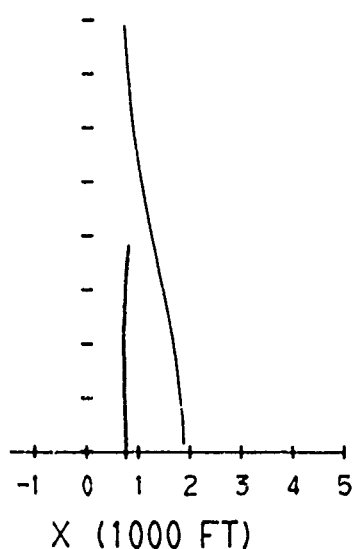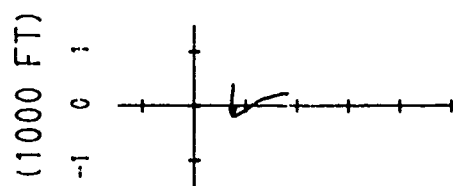
4,000 FT TOWED CABLE — — — — —

Figure 13b

Figure 13c
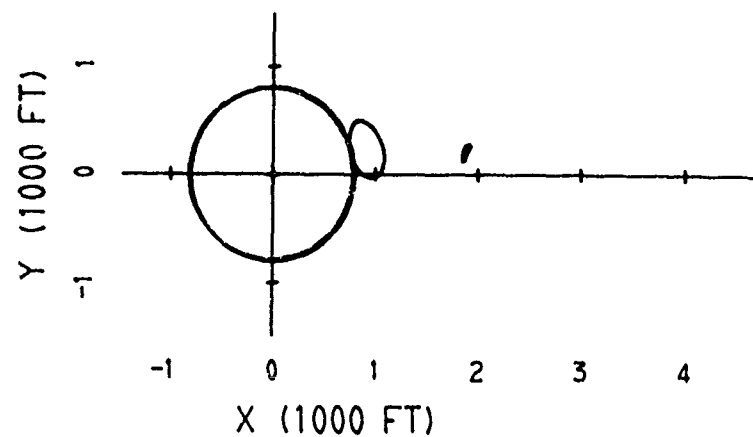
Figure 13d

Figure 13e

64
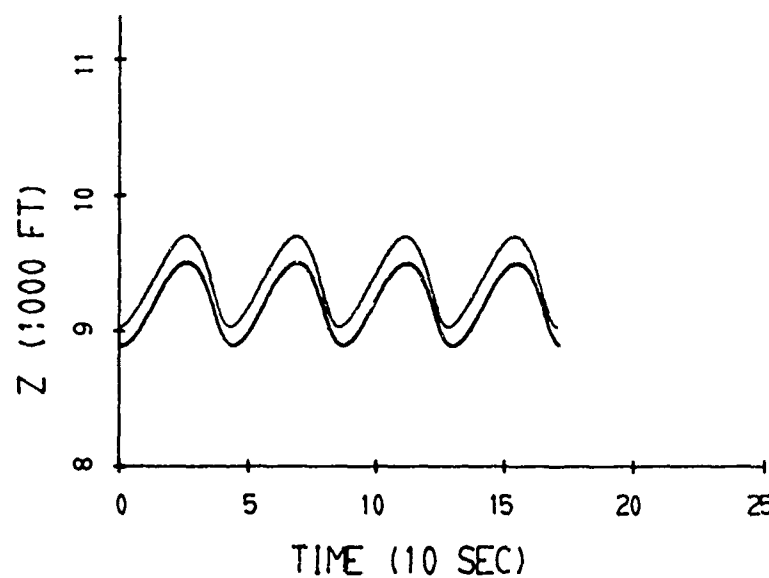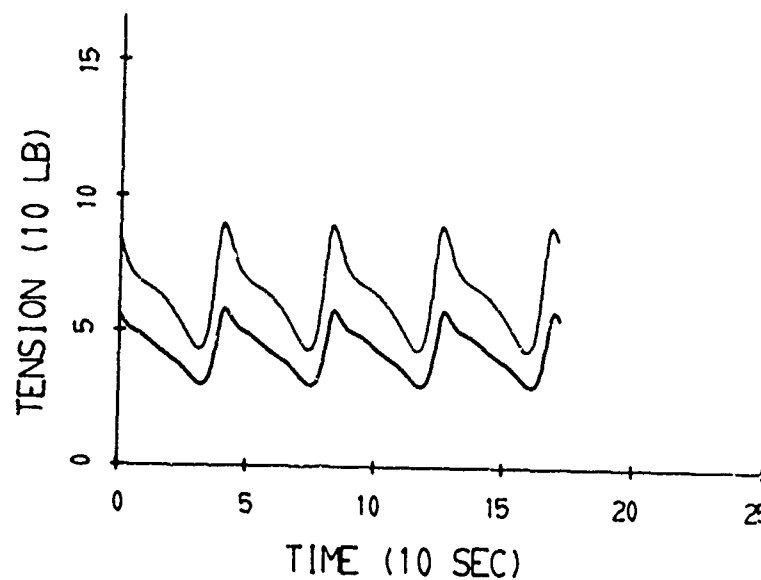
CASE 8

CIRCULAR FLIGHT PATH

15 KTAS CONSTANT WIND VELOCITY PROFILE

Figure 14a

8,000 FT TOWED CABLE
DROGUE WEIGHT = 100 LB

8,000 FT TOWED CABLE
DROGUE WEIGHT = 25 LB
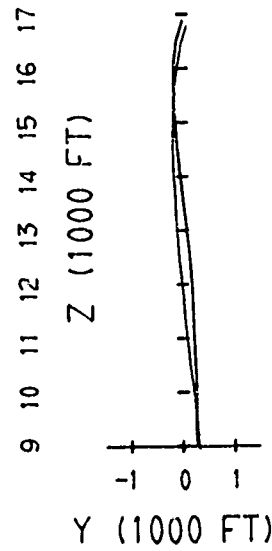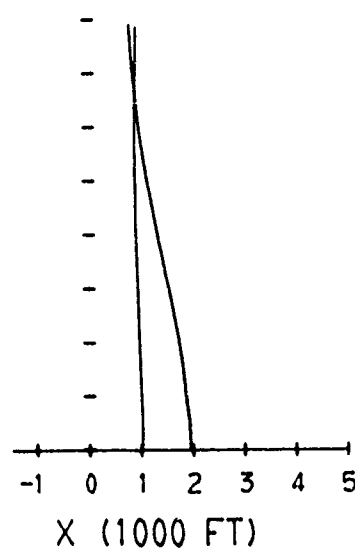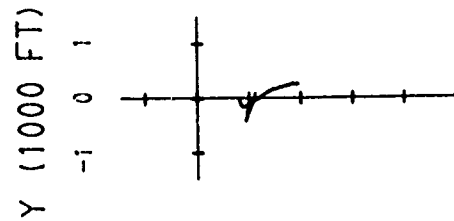
Figure 14b

Figure 14c

Y (1000 FT)

X (1000 FT)

Figure 14d

Z (1000 FT)

TIME (10 SEC)

Figure 14e

TENSION (10 LB)

TIME (10 SEC)

66
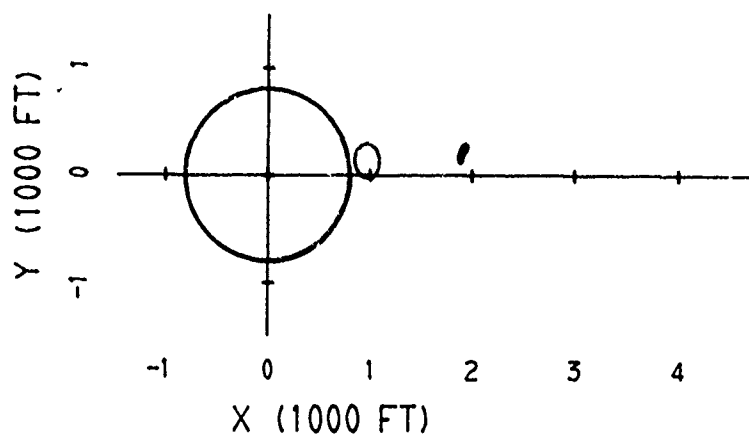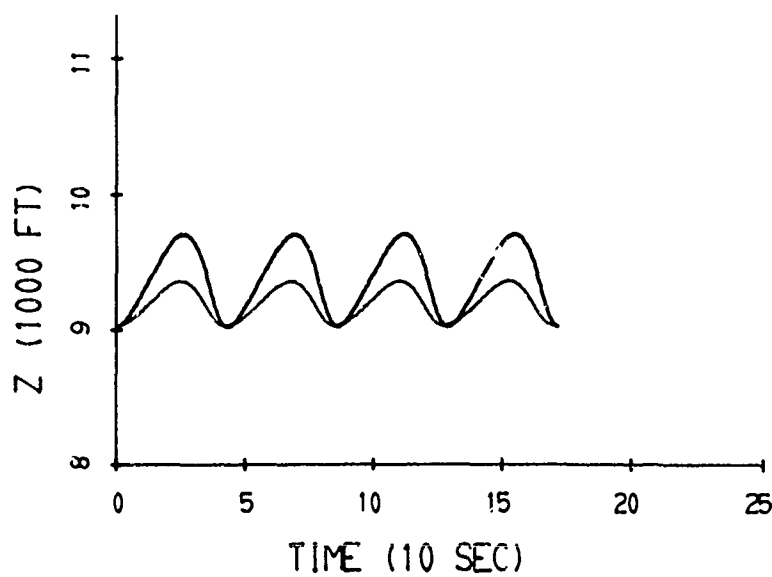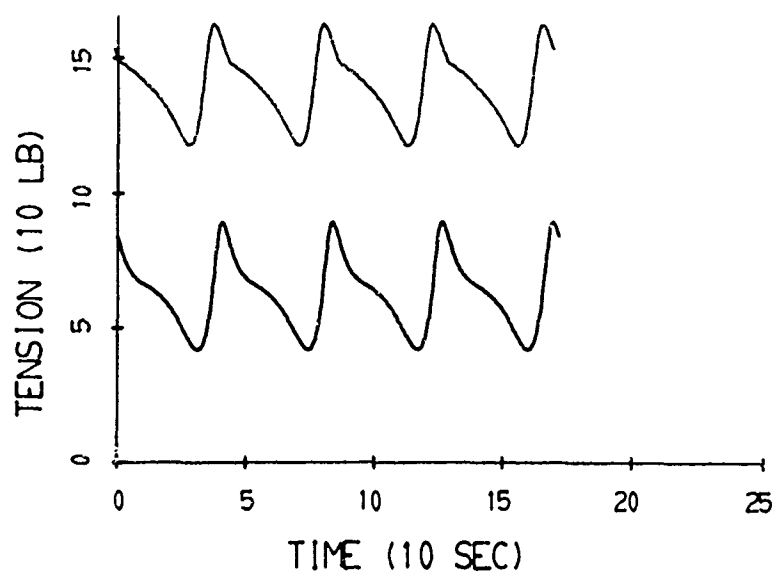
CASE 9

TILTED ELLIPTICAL FLIGHT PATH
AND LEVEL CIRCULAR FLIGHT PATH

15 KTAS CONSTANT WIND VELOCITY PROFILE

8,000 FT TOWED CABLE (TILTED)   ———

8,000 FT TOWED CABLE (LEVEL)   ———
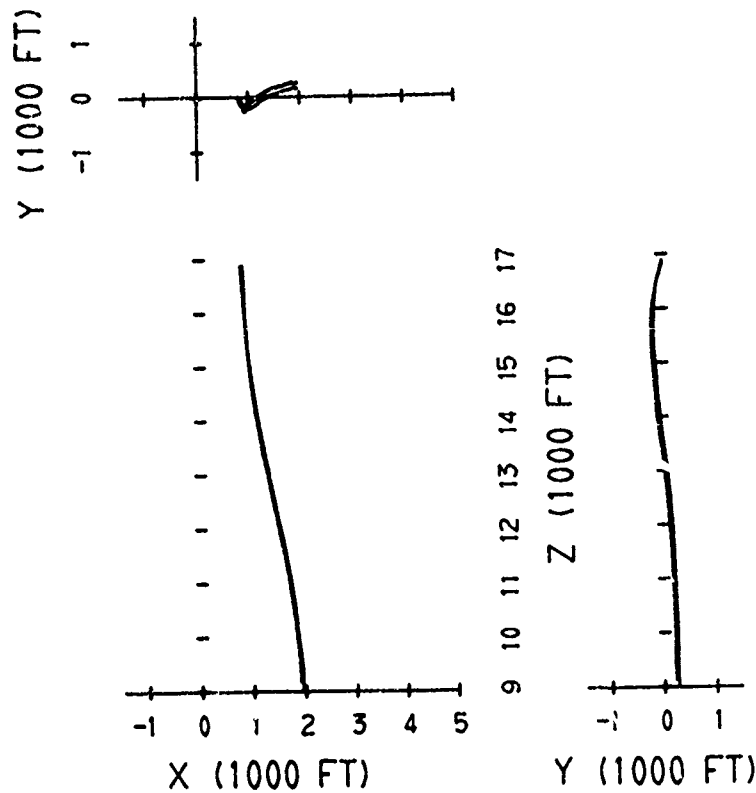
Figure 15c
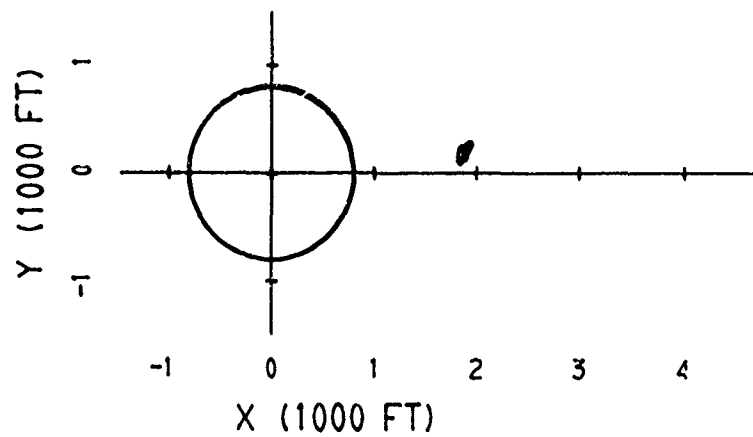
Figure 15d
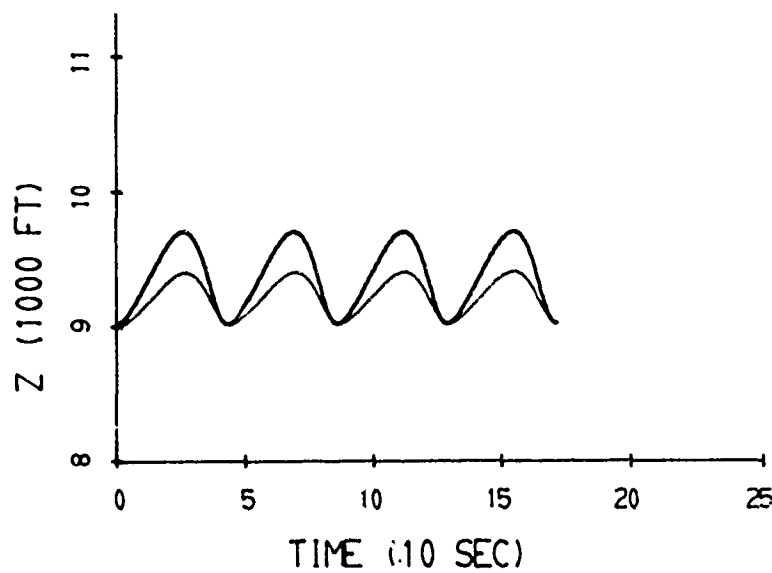
Figure 15e
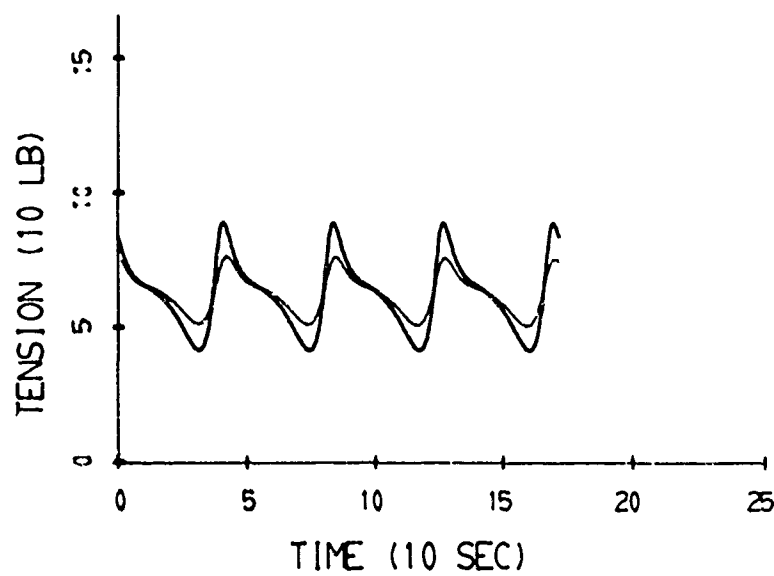
CASE 10

CIRCULAR FLIGHT PATH

Figure 16a

8,000 FT TOWED CABLE   ———————
15 KTAS POWER LAW WIND VELOCITY PROFILE

8,000 FT TOWED CABLE   ———————
15 KTAS CONSTANT WIND VELOCITY PROFILE

Figure 16b

69

Figure 16c

Figure 16d

Figure 16e

70
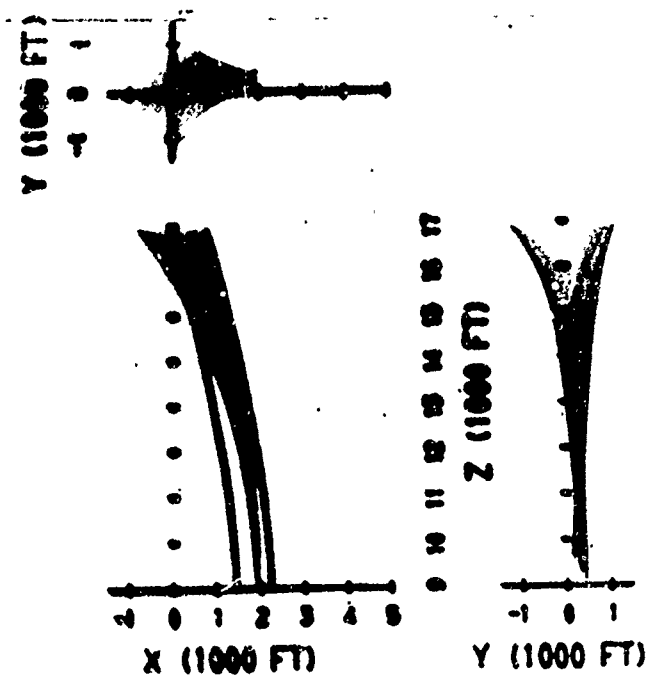
Figure 18

Figure 19

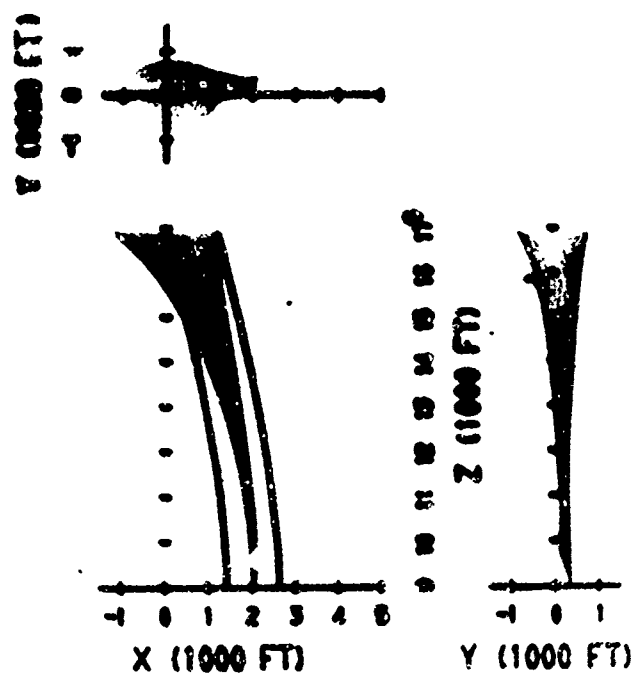71
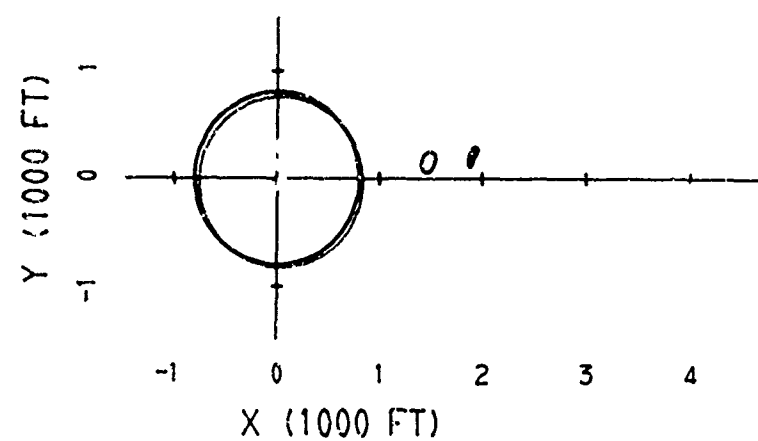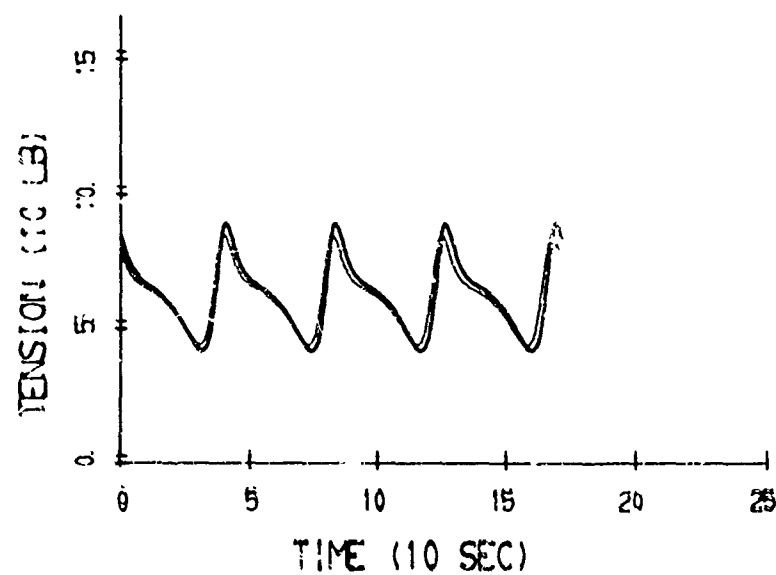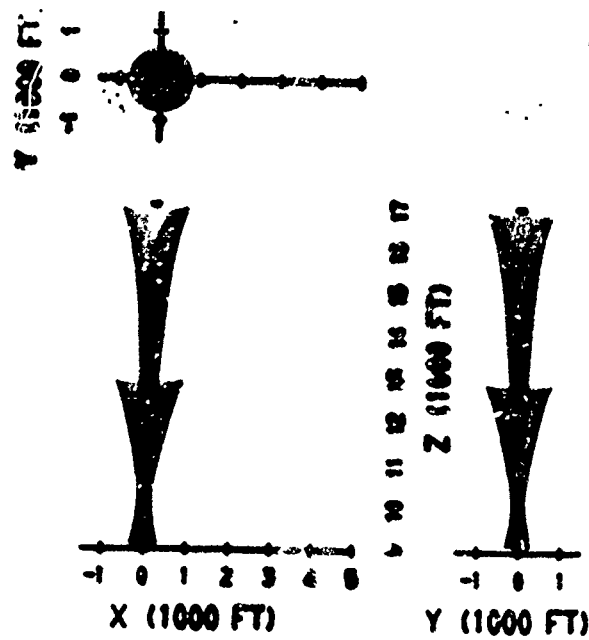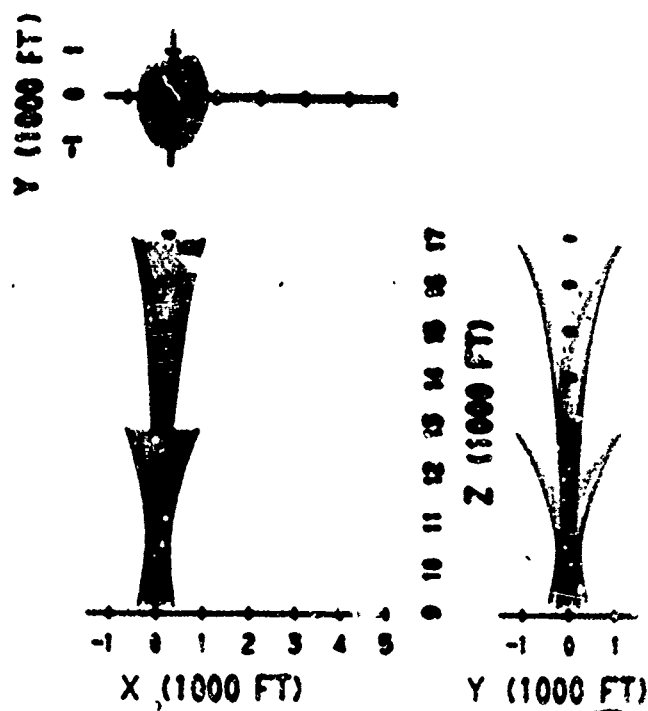
Figure 20

Figure 21

72
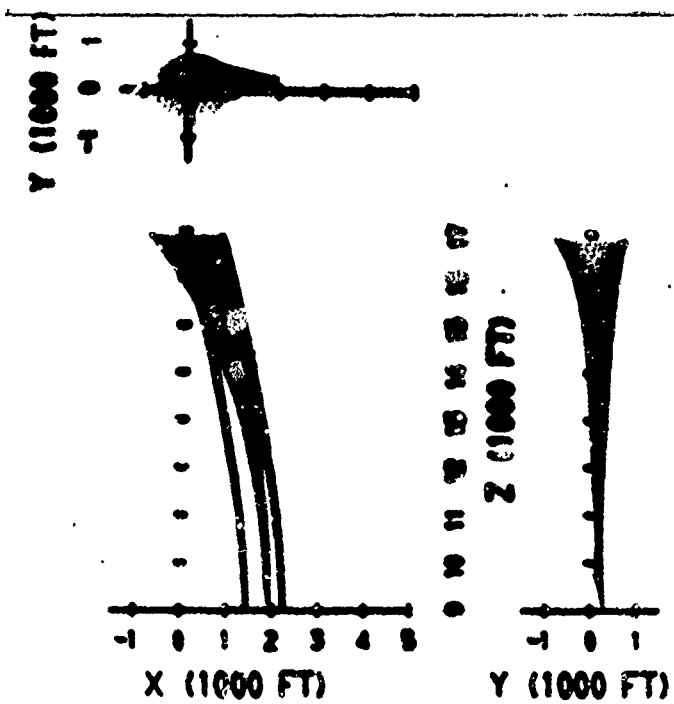
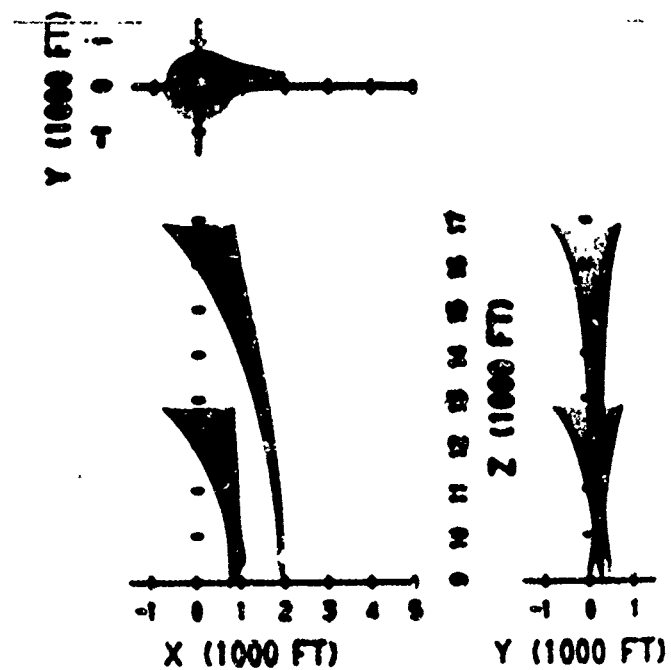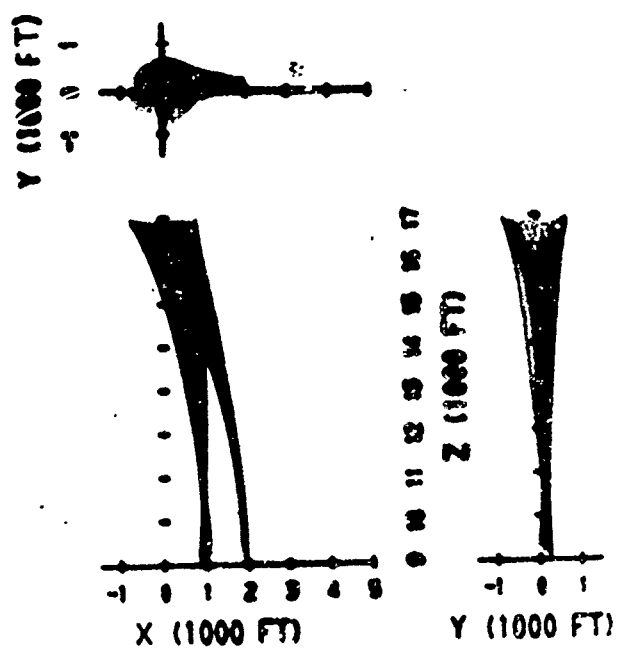Figure 22

Figure 23

73

Figure 24

Figure 25

74
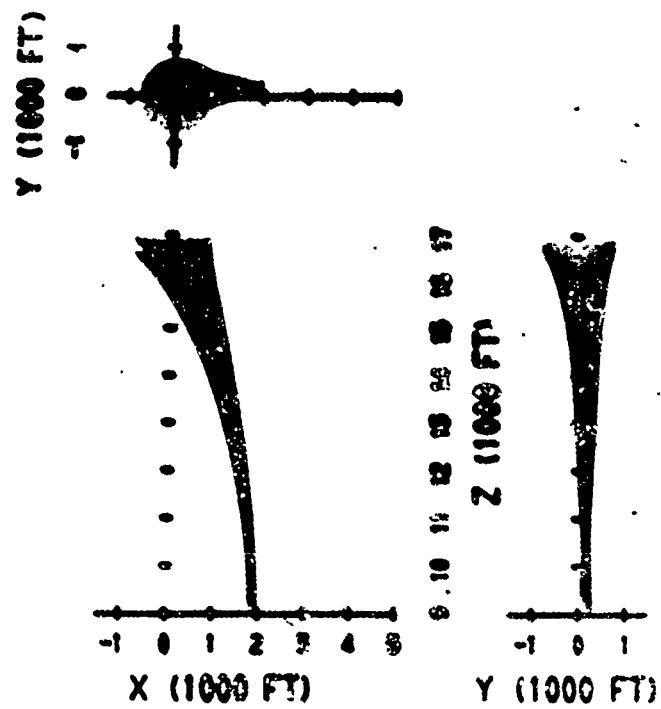
Figure 26

LIST OF REFERENCES

1. Casarella, M. J. and Parsons, M. "Cable Systems Under Hydrodynamic Loading." MTS Journal, Volume 4, Number 4, July-August 1970, pp. 27-44.

2. Hinnerichs, T. D., Crist, S. A., "Steady State Shape of Orbiting Trailing Wire System", USAFA Research Report 72-7, 1972.

3. Crouch, J. G., Bauer, P. T. an- Kahle, D. A. "An Analytic Study of the Requirements for an Automatic Long-Line System." Technical Report UDRI-TR-70-31, July 1970.

4. Liller, J. C., "Analysis of the Dynamic Motion of a Circling Line in the Presence of Winds and Gusts." Thesis GA/MC/69-5, June 1969.

5. NACA Standard Atmosphere Tables

6. Hansen, J. G., "Trailing Wire Antenna Configurations Using Snowbird Cable Towed by U-10 Aircraft", Film #C-3397, Alexander Film Services, Colorado Springs, Colorado, 1971.

APPENDIX I

The cable is divided into n mass points connected by straight, linear elastic, massless segments. If an adequate number of mass points are taken, the model accurately predicts the response of the actual cable. Each mass point has three degrees of freedom and is located in the x, y, z coordinate system shown in Figure 27.

The equations of motion can be derived using Lagrange's Equation and treating the aerodynamic forces as generalized forces. The kinetic energy of the cable system is given by

$$T = \sum_{i=1}^{n} \frac{m_i}{2} (\dot{x}_i^2 + \dot{y}_i^2 + \dot{z}_i^2). \tag{1}$$

the potential energy is given by

$$V = \sum_{i=1}^{n} \frac{k_i}{2} (e_i - s_{o_i})^2 + \sum_{i=1}^{n} m_i g z_i \tag{2}$$

where m_i = mass of ith point

k_i = spring constant for segment

e_i = stretched spring length

s_{o_i} = unstretched spring length

$g = 32.3$ ft/sec^2.

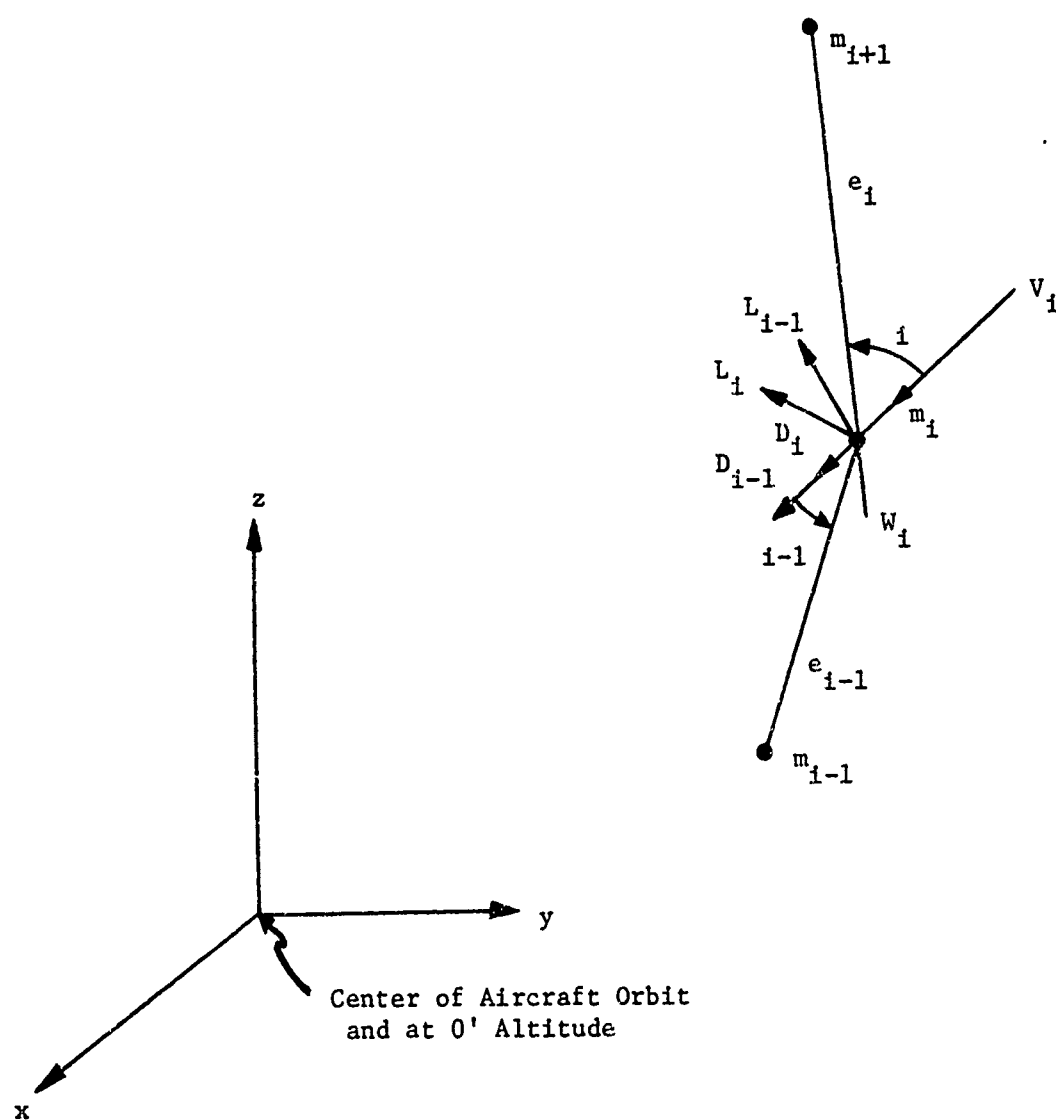For any given mass point, i, the two connecting segments e_i and e_{i+1} are given by

77

FIGURE 27

COORDINATE SYSTEM FOR i^{th} MASS POINT

78

In addition

$$\frac{\partial e_i}{\partial q_i} = -\frac{(q_{i+1}-q_i)}{e_i} \quad \text{and} \quad \frac{\partial e_{i-1}}{\partial q_i} = \frac{(q_i-q_{i-1})}{e_{i-1}}$$

where again the q_i's are x_i, y_i or z_i.

The last step is to calculate the Q_i forces due to lift and drag on each cable segment. The wind velocity vector, $\vec{V}_i$, is due to the cable motion and can be expressed as

$$\vec{V}_i = -\dot{x}_i \,\hat{i} - \dot{y}_i \,\hat{j} - \dot{z}_i \,\hat{k} . \tag{8}$$

the vectors along the e_i and e_{i-1} segments can be expressed as

$$\bar{e}_i = (x_{i+1} - x_i)\,\hat{i} + (y_{i+1}-y_i)\,\hat{j} + (z_{i+1}-z_i)\,\hat{k} \tag{9}$$

and

$$\bar{e}_{i-1} = (x_i-x_{i-1})\,\hat{i} + (y_i-y_{i-1})\,\hat{j} + (z_i-z_{i-1})\,\hat{k} .$$

From the dot product, the angles of attach, β_i and β_{i-1} can be found to be given by

$$\beta_i = \cos^{-1}\left\{\frac{-\bar{V}_i \cdot \bar{e}_i}{|V_i||e_i|}\right\} \tag{10} \quad \text{and} \quad \beta_{i-1} = \cos^{-1}\frac{-\bar{V}_i \cdot \bar{e}_{i-1}}{|\bar{V}_i||\bar{e}_{i-1}|} . \tag{11}$$

From the cross products one can find the vectors in the direction of lift (i.e. perpendicular to $\bar{V}_i$ and in the plane formed by $\bar{V}_i$ and $\bar{e}_i$ or $\bar{e}_{i-1}$). Letting $\hat{\eta}_i$ and $\hat{\eta}_{i-1}$ be unit vectors in the lift direction we get

$$\hat{\eta}_i = \frac{(\bar{V}_i \times \bar{e}_i) \times \bar{V}_i}{|(\bar{V}_i \times \bar{e}_i) \times \bar{V}_i|} \tag{12} \quad \text{and} \quad \hat{\eta}_{i-1} = \frac{(\bar{V}_i \times \bar{e}_{i-1}) \times \bar{V}_i}{|(\bar{V}_i \times \bar{e}_{i-1}) \times \bar{V}_i|} \tag{13}$$

79

$$e_i = \sqrt{(x_{i+1} - x_i)^2 + (y_{i+1} - y_i)^2 + (z_{i+1} - z_i)^2} \tag{3}$$

and

$$e_{i-1} = \sqrt{(x_i - x_{i-1})^2 + (y_i - y_{i-1})^2 + (z_i - z_{i-1})^2} \tag{4}$$

The Lagrangian is given by $L = T-V$ and Lagrange's equation of motion is

$$\frac{d}{dt}\left[\frac{\partial L}{\partial \dot{q}_i}\right] - \frac{\partial L}{\partial q_i} = Q_i \tag{5}$$

where the q_i are the generalized coordinates, namely x_i, y_i and z_i and the Q_i are the generalized forces arising from the lift and drag.

The derivatives indicated by Equation (5) are as follows

$$\frac{d}{dt}\left[\frac{\partial L}{\partial \dot{q}_i}\right] = \begin{cases} m_i \, \ddot{x}_i \\ m_i \, \ddot{y}_i \\ m_i \, \ddot{z}_i \end{cases} \tag{6}$$

and

$$\frac{\partial L}{\partial q_i} = \begin{cases} -k_i(e_i - S_{o_i})\dfrac{\partial e_i}{\partial x_i} - k_{i-1}(e_{i-1} - S_{o_{i-1}})\dfrac{\partial e_{i-1}}{\partial x_i} \\[2ex] -k_i(e_i - S_{o_i})\dfrac{\partial e_i}{\partial y_i} - k_{i-1}(e_{i-1} - S_{o_{i-1}})\dfrac{\partial e_{i-1}}{\partial y_i} \\[2ex] -k_i(e_i - S_{o_i})\dfrac{\partial e_i}{\partial z_i} - k_{i-1}(e_{i-1} - S_{o_{i-1}})\dfrac{\partial e_{i-1}}{\partial z_o} - m_i g \end{cases} \tag{7}$$

for $q_i = x_i$, y_i and z_i respectively.

80

$$- m_i g + L_i \eta_{z_i} + L_{i-1} \eta_{z_{i-1}} + (D_i + D_{i-1}) \xi_{z_i} \quad i = 1, \ldots, n.$$

In the above equations, η_x, η_y, η_z, ϵ_x, ϵ_y, ϵ_z are the direction cosines of vectors $\hat{\eta}$ and $\hat{\epsilon}$, respectively.